Recent tests of the EW sector with ATLAS

Observation of EW production of WZ and same-sign WW at 13 TeV (36 fb^{-1})

and

Measurement of $\sin^2\theta^l_{eff}$ at 8 TeV

Presented by D. Froidevaux

on behalf of the ATLAS collaboration

Recent tests of the EW sector with ATLAS

Precise tests of the EW sector in the SM at the LHC require efforts in two different directions:

a) **Tests of the consistency of the SM through higher precision measurements of its fundamental parameters. This requires specific efforts in the experimental community and the theory community**
   - **low-μ runs in 2017/2018 to measure precisely p_T^W**
   - **precision DY measurements require ultimate performance of detector for electrons/muons and hadronic recoil**
   - **improve theoretical predictions and uncertainty estimates for p_T^W/p_T^Z**
   - **using high $|y^{ll}|$ events to enhance sensitivity to weak mixing angle**
   - **validate use of improved Born approximation at the LHC for precision Z physics**

b) **Tests of the consistency of the SM through direct exploration of the EW symmetry breaking mechanism using diboson production. This requires eventually very large datasets (HL-LHC or beyond) and specific efforts from the theory community**
   - **observation and differential measurements of EW processes**
   - **higher-order calculations of diboson EW production, existing to-date only for same-sign WW EW production**

LPCC SM working group is quite active in promoting dedicated work between experiments and theory on all these fronts (see later slide).

Precision tests of the EW sector

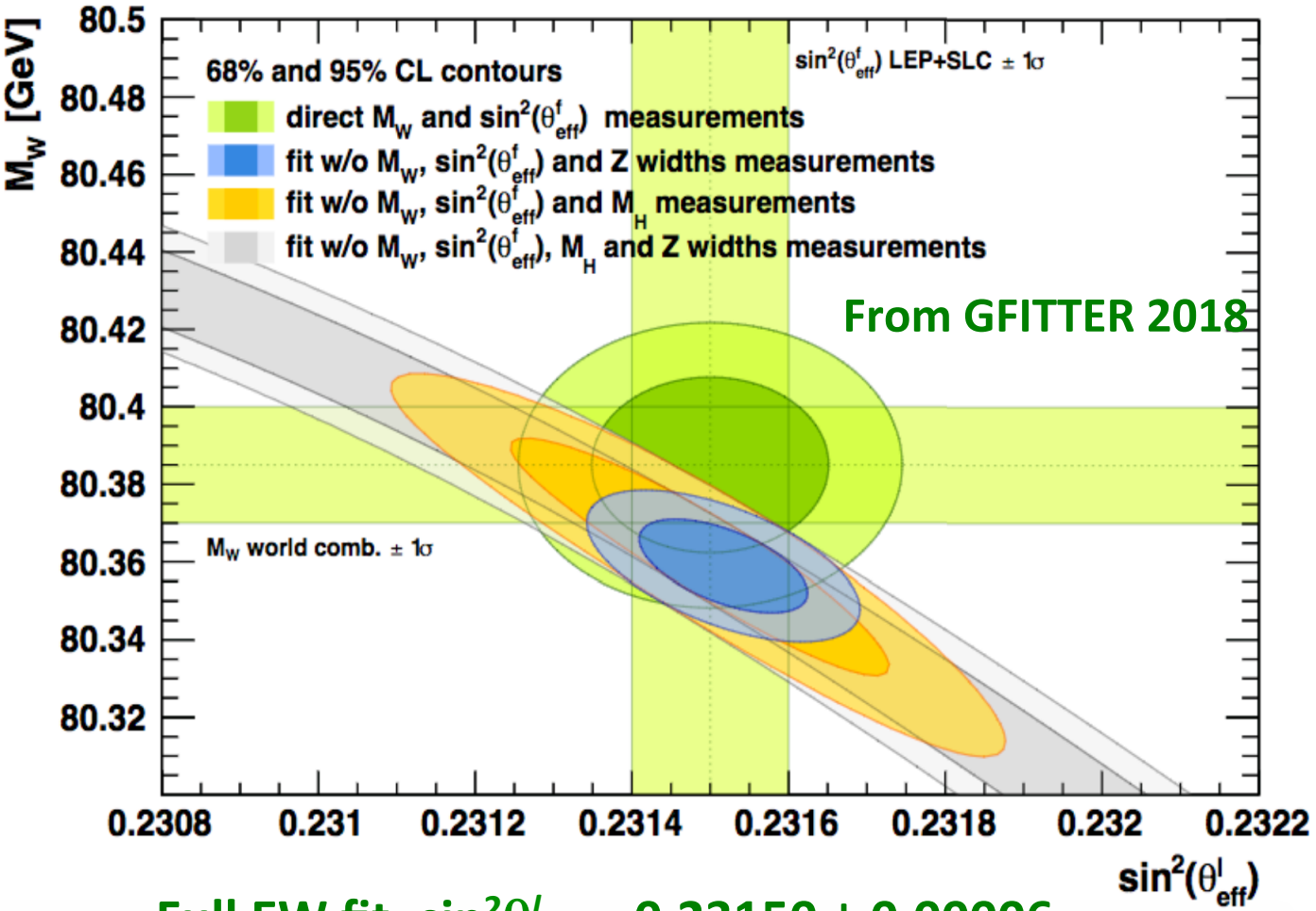

Full EW fit: $\sin^2\theta^l_{eff} = 0.23150 \pm 0.00006$

Indirect determination from EW fit: $\sin^2\theta^l_{eff} = 0.23149 \pm 0.00007$

Lepton collider average (LEP/SLC): $\sin^2\theta^l_{eff} = 0.23152 \pm 0.00016$

ATLAS measurement of $\sin^2\theta^l_{eff}$ at 8 TeV

$\sin^2\theta^l_{eff} = 0.23140 \pm 0.00021\,(\text{stat.}) \pm 0.00024\,(\text{PDF}) \pm 0.00016\,(\text{syst.})$

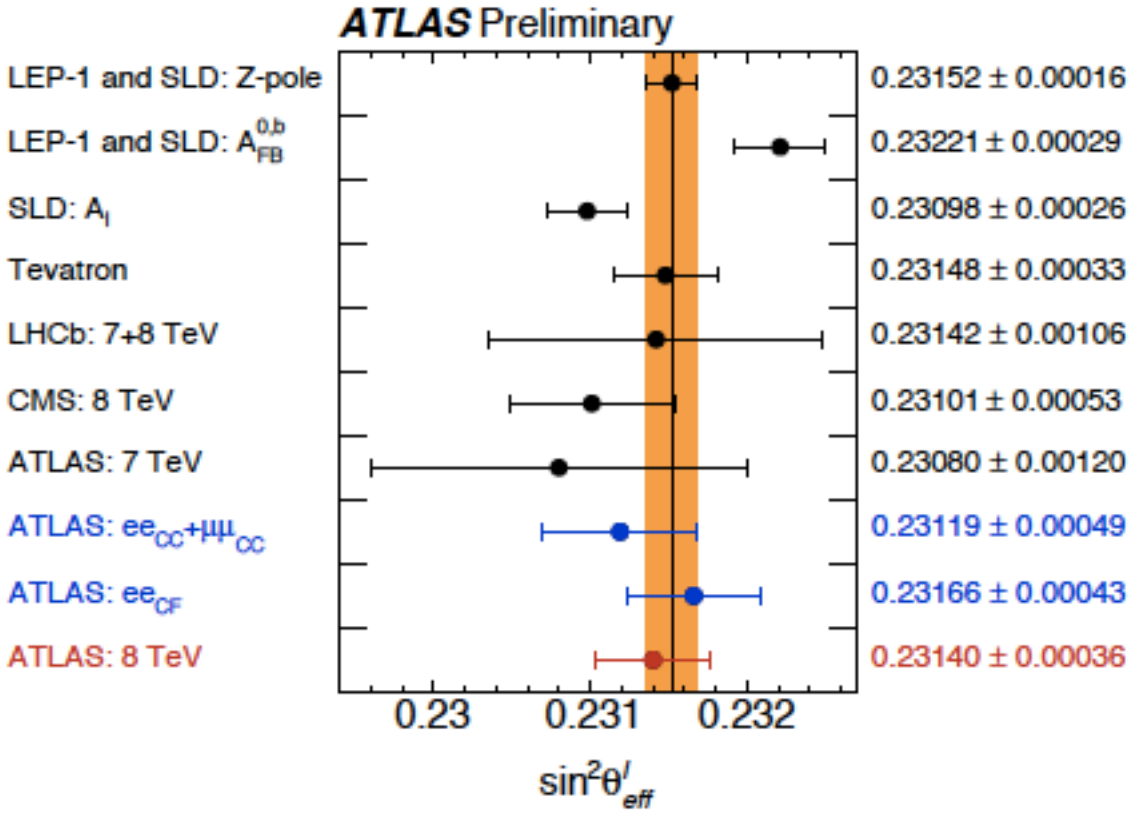

Links to papers and to preliminary result on $\sin^2\theta^l_{eff}$:

- Angular coefficients in Z-boson decays at 8 TeV
- Triple-differential measurements of Z-boson decays at 8 TeV
- Measurement of $\sin^2\theta^l_{eff}$ at 8 TeV

Observation of WZ and same-sign WW EW processes

- **WZ EW observed at 5.6σ (3.3σ expected from Sherpa)**
- **Same-sign WW EW observed at 6.9σ (4.6σ expected from Sherpa)**
- **More importantly, fiducial and differential cross-section measurements are performed**
- **Also, beautiful results from inclusive WZ measurements with first measurements of longitudinal and transverse polarisation of W and Z bosons in diboson production**

Links to preliminary results:

- **WZ electroweak observation at 13 TeV (36 fb^{-1})**
- **Same-sign WW EW observation at 13 TeV (36 fb^{-1})**
- **WZ differential and polarisation measurements at 13 TeV (36 fb^{-1})**

Observation of WZ and same-sign WW EW processes

- **Examples of VVjj EW VBS diagrams, these are all o(α^6)**

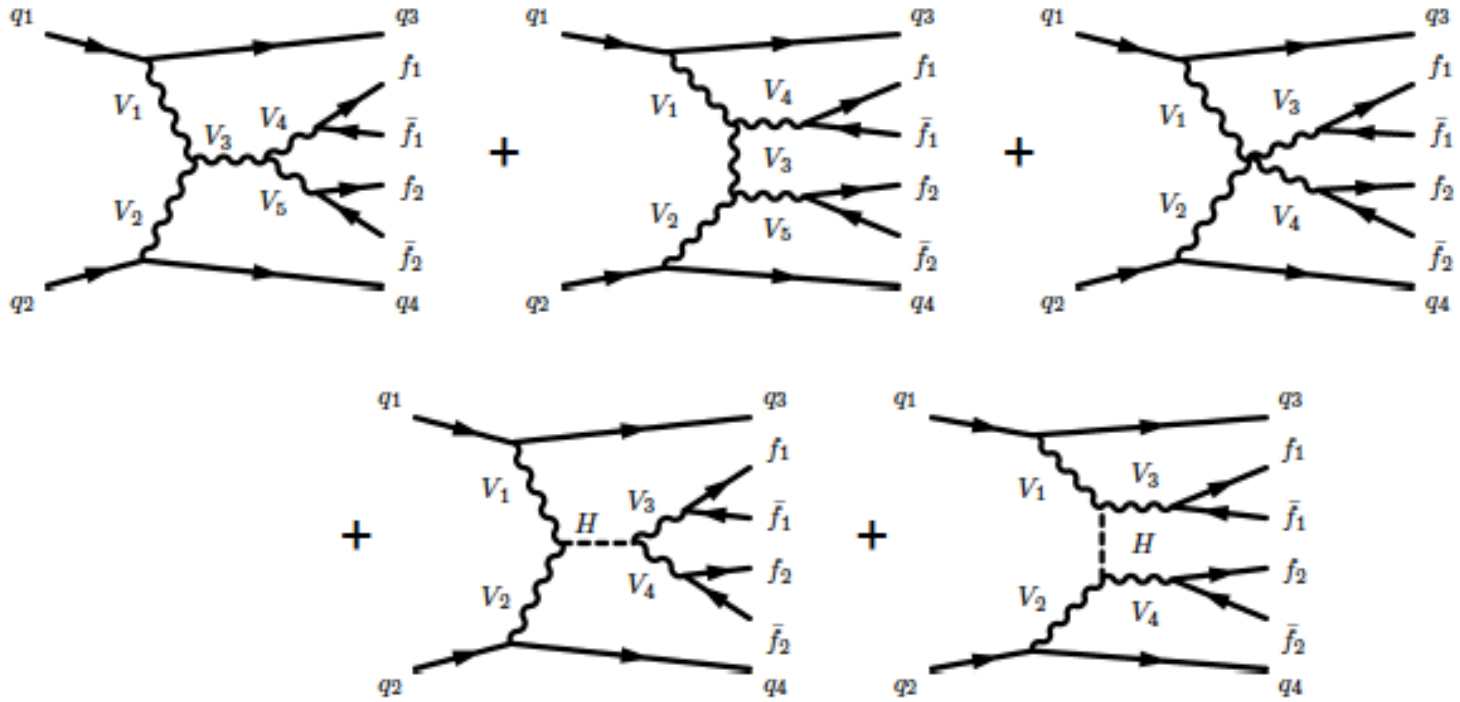

Figure 1: Representative Feynman diagrams for VVjj-EW production with a scattering topology including either a triple gauge boson vertex with production of a W/Z boson in the s-channel (top left diagram), the t-channel exchange (top middle diagram), quartic gauge boson vertex (top right diagram), or the exchange of a Higgs boson in the s-channel (bottom left diagram) and t-channel (bottom right diagram). The lines are labeled by quarks (q), vector bosons ($V = W, Z$), and fermions (f).

Observation of WZ and same-sign WW EW processes

- **Examples of VVjj EW non-VBS diagrams, these are all o(α^6)**

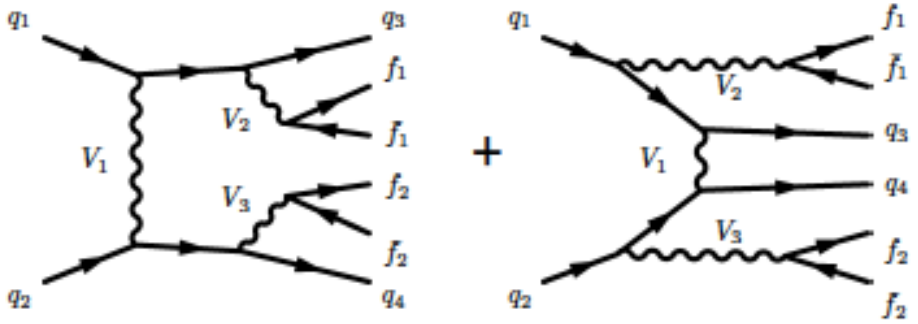

Figure 2: Representative Feynman diagrams for VVjj-EW production without vector-boson scattering topology. The lines are labeled by quarks (q), vector bosons ($V = W, Z$), and fermions (f).

- **Examples of VVjj QCD diagrams, these are all o($\alpha^4\alpha_s^2$)**

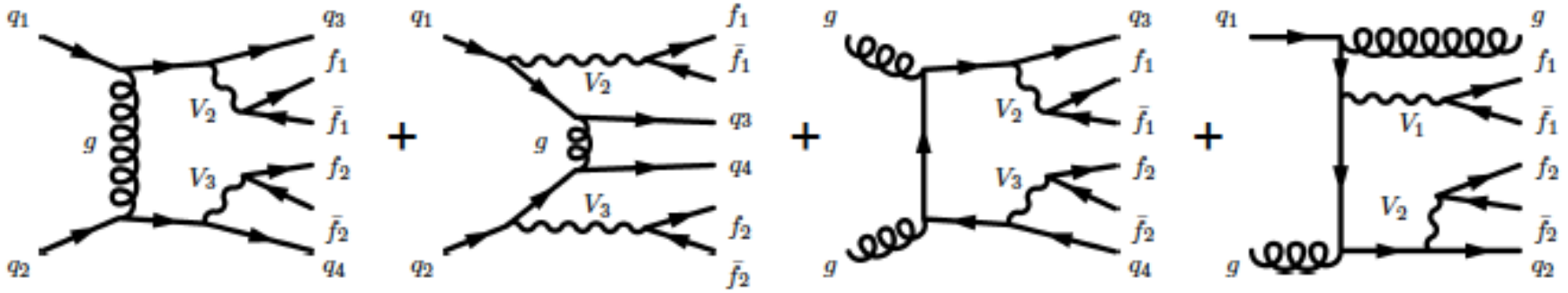

Figure 3: Representative Feynman diagrams for VVjj-QCD production defined by VBS topologies with strong interaction vertices. The lines are labeled by quarks (q), vector bosons ($V = W, Z$), fermions (f), and gluons (g).

Observation of WZ and same-sign WW EW processes

WZjj VBS selection

- Leptons Z $p_T > 15$ GeV, $|\eta| < 2.5$
  Lepton W $p_T > 20$ GeV, $|\eta| < 2.5$
  $m_T^{l\nu} > 30$ GeV, $\Delta R_{ll} > 0.3$
  Medium selection
- Jets: $p_T^{1,2} > 40$ GeV, $|\eta| < 4.5$
  b-jet veto
- Signal region (SR):
  $m_{jj} > 500$ GeV + high BDT score
- Dominant background:
  - WZjj QCD (144 events prefit):
    use CR with $200 < m_{jj} < 500$ GeV
  - Misid. and ZZjj ~ factor 10 lower
- Expected signal: 25 events (Sherpa)
- S/B in SR: ~ 14% prefit / 38% post-fit

Same-sign WWjj VBS selection

- Leptons: $p_T > 27$ GeV, $|\eta| < 2.5$
  $m_{ll} > 20$ GeV, $\Delta R_{ll} > 0.3$
  Tight selection plus isolation
- Jets: $p_T^{1,2} > 65, 35$ GeV, $|\eta| < 4.5$
  b-jet veto
- Signal region (SR):
  $m_{jj} > 500$ GeV, $|\Delta y_{jj}| > 2.0$
  Categorisation and bins in m_{jj}
- Dominant background:
  - Misid. and $V\gamma$ (36 events prefit)
  - WWjj QCD lower (7 events):
    use CR with $200 < m_{jj} < 500$ GeV
- Expected signal: 41 events (Sherpa)
- S/B in SR: ~ 50-55% prefit/post-fit

Observation of WZ EW process

- BDT trained to separate WZ EW signal from all other processes (except misid. leptons)
- Good description of BDT shape in WZjj QCD control region (below left)
- In signal region (below right), the WZjj EW signal dominates for high values of the BDT score → clear observation of signal and way open to measure fiducial differential cross sections

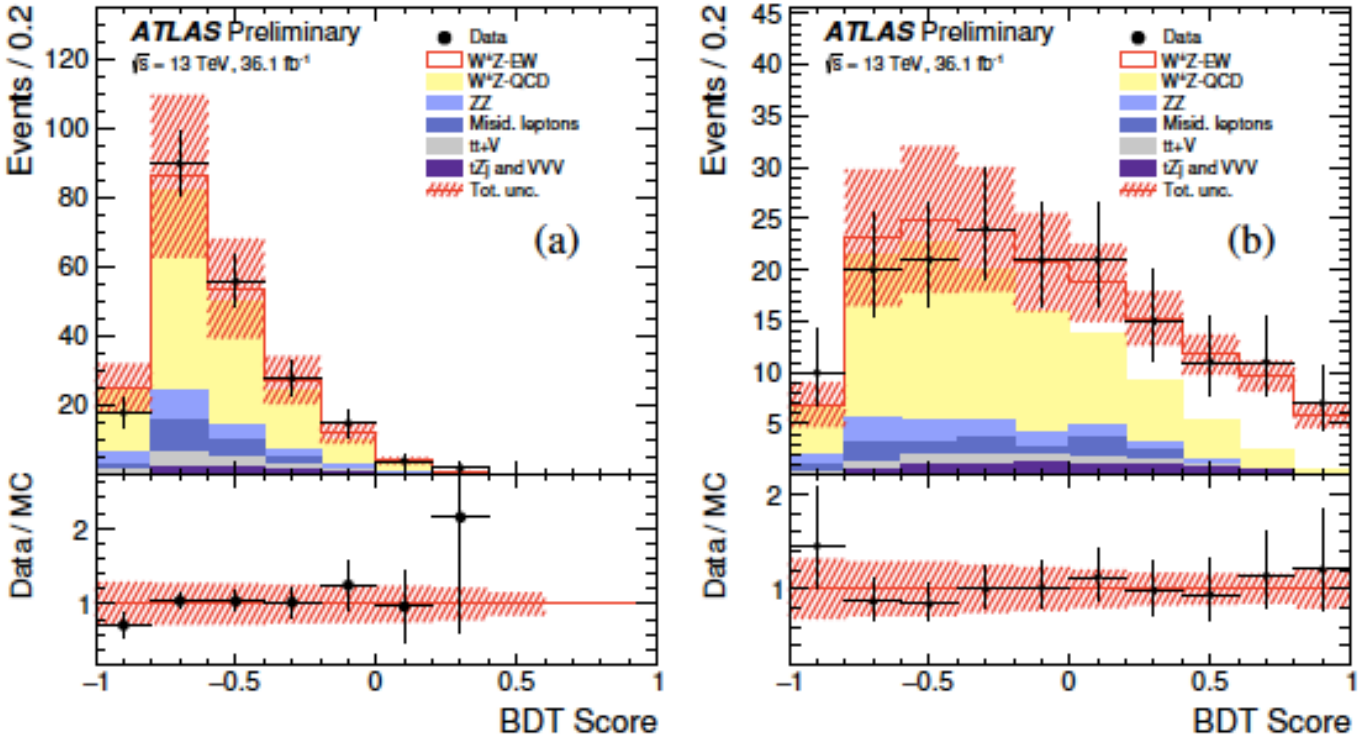

Figure 1: Post-fit BDT score distributions in the QCD control region (a) and in the signal region (b). Signal and backgrounds are normalised to the expected number of events after the fit. The uncertainty band around the MC expectation includes the systematic uncertainties as obtained by the fit.

Observation of WZ EW process
Fiducial cross section

- **WZjj EW :** $\sigma_{meas.}^{\text{fid., EW}} = 0.57\ ^{+0.14}_{-0.13}\,(\text{stat.})\ ^{+0.05}_{-0.04}\,(\text{syst.})\ ^{+0.04}_{-0.03}\,(\text{th.})\ \text{fb}$

- **What about predictions?** **Sherpa v2.2.2:** **0.32 ± 0.03 fb**

- **Only LO predictions exist for WZjj EW production.**

Observation of WZ EW process

- **Examples of differential distributions for WZ EW signal region:**
  Δy_{jj} (left) and m_{jj} (right), compared to Sherpa predictions rescaled to their post-fit values.

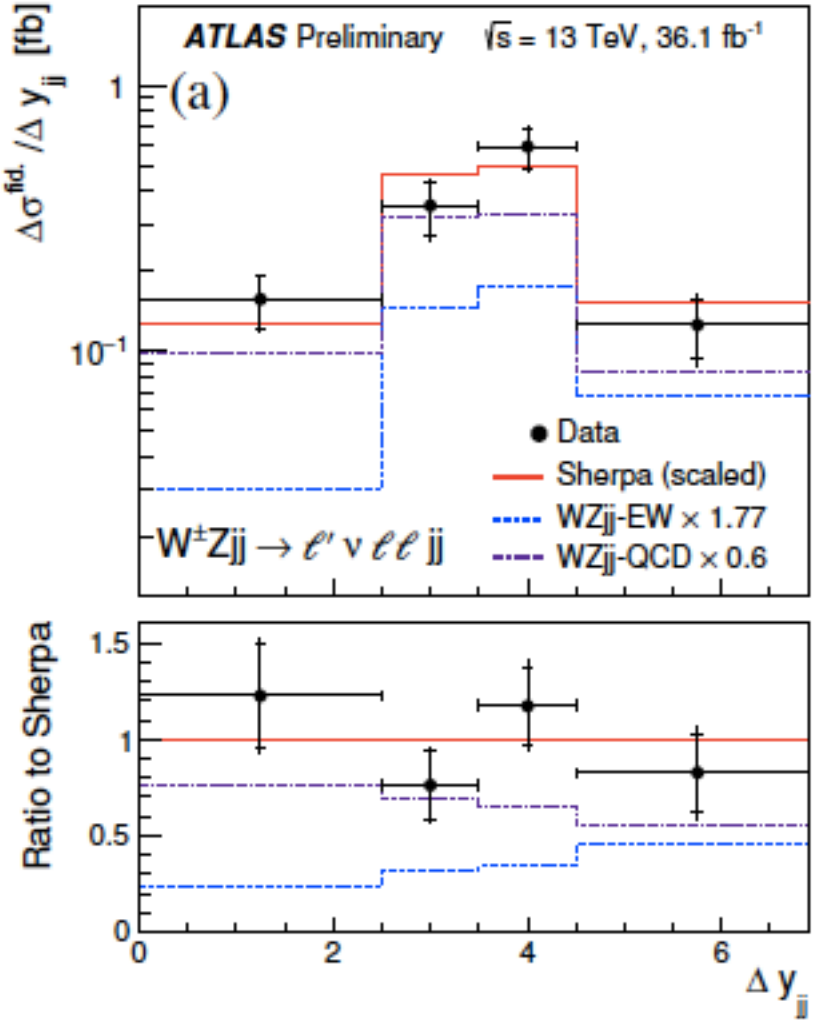

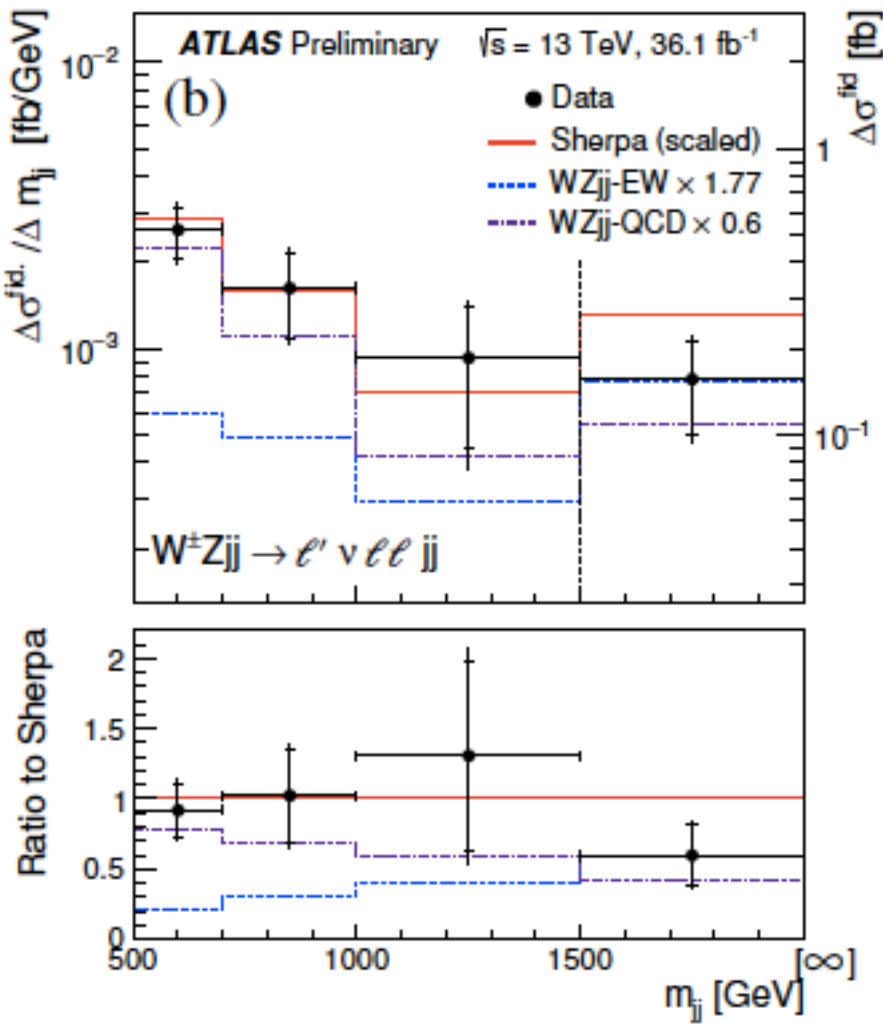

Observation of WZ EW process

- Examples of differential distributions for WZ EW signal region and for WZ inclusive measurements: number of additional jets observed (in gap for WZ EW)
- Comparison is to Sherpa predictions rescaled to their post-fit values for WZ EW
- Comparisons are to Sherpa 2.2.2 and 2.1 and to Powheg+Pythia for WZ inclusive

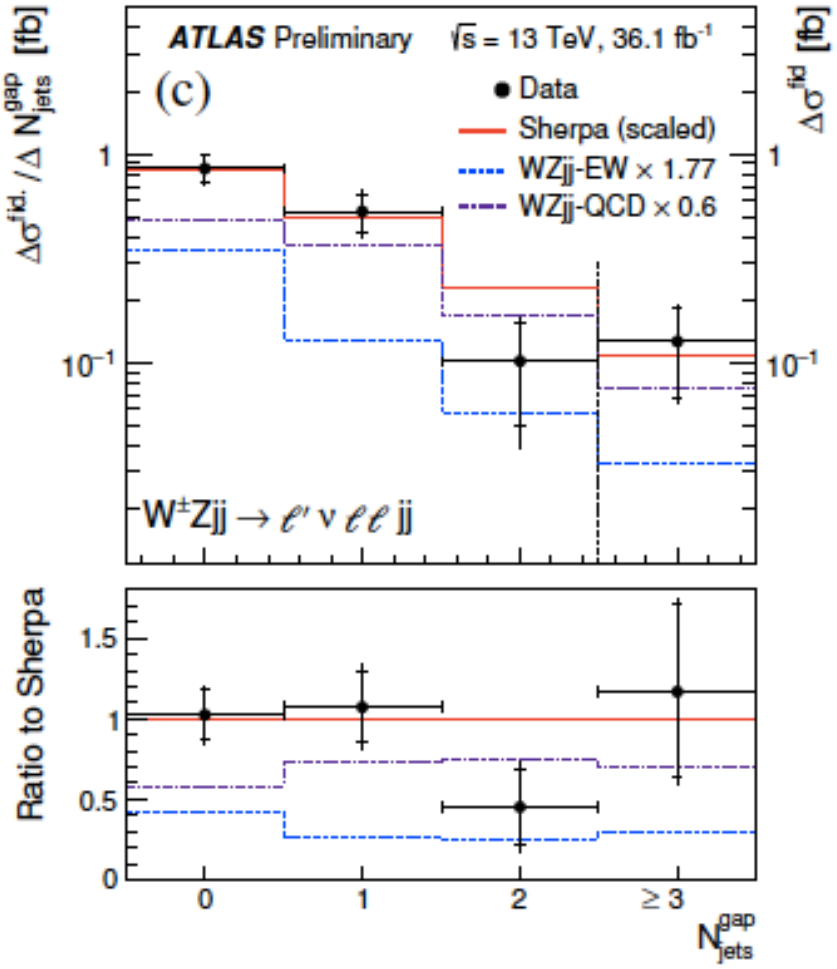

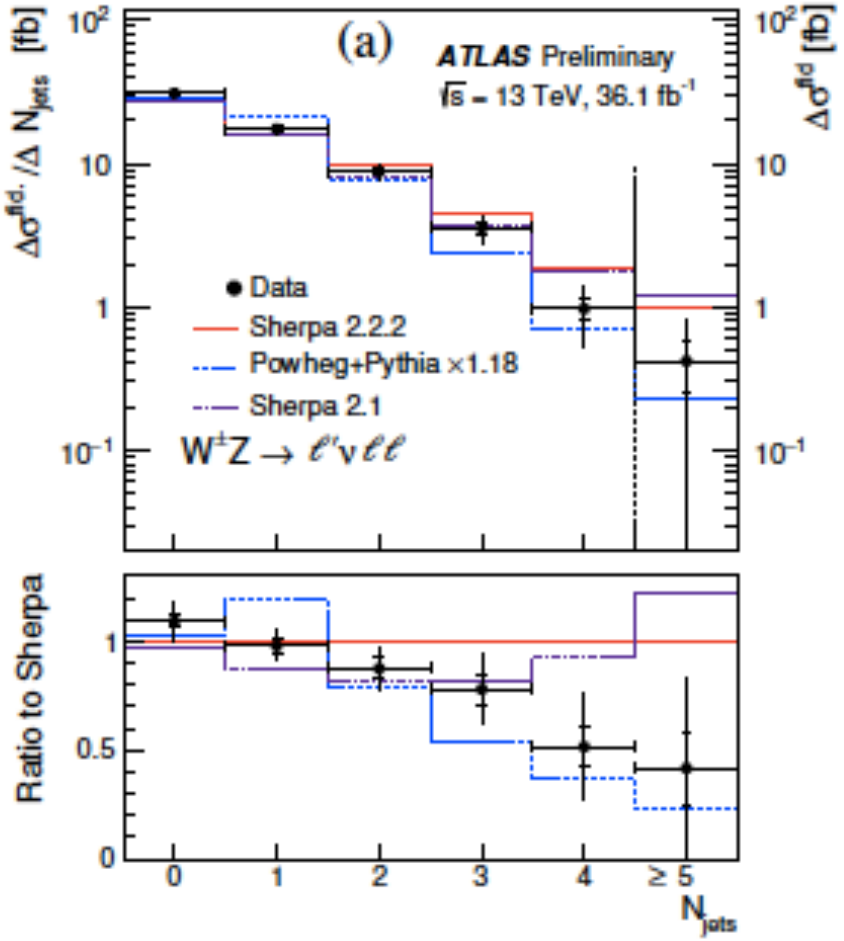

First measurement of W/Z polarisation in diboson processes

- Helicity fractions f_0 (longitudinal polarisation) and f_L/f_R (transverse polarisation)
- Evidence for longitudinally polarised Ws at 4.2σ (3.8σ expected)
- Theory predictions are LO EW with $\sin^2\theta_W = 0.23152$ (PDG 2016)

$$\frac{1}{\sigma_{W^\pm Z}}\frac{d\sigma_{W^\pm Z}}{d\cos\theta_{\ell,W}} = \frac{3}{8}f_L(1\mp\cos\theta_{\ell,W})^2 + \frac{3}{8}f_R(1\pm\cos\theta_{\ell,W})^2 + \frac{3}{4}f_0\sin^2\theta_{\ell,W}$$

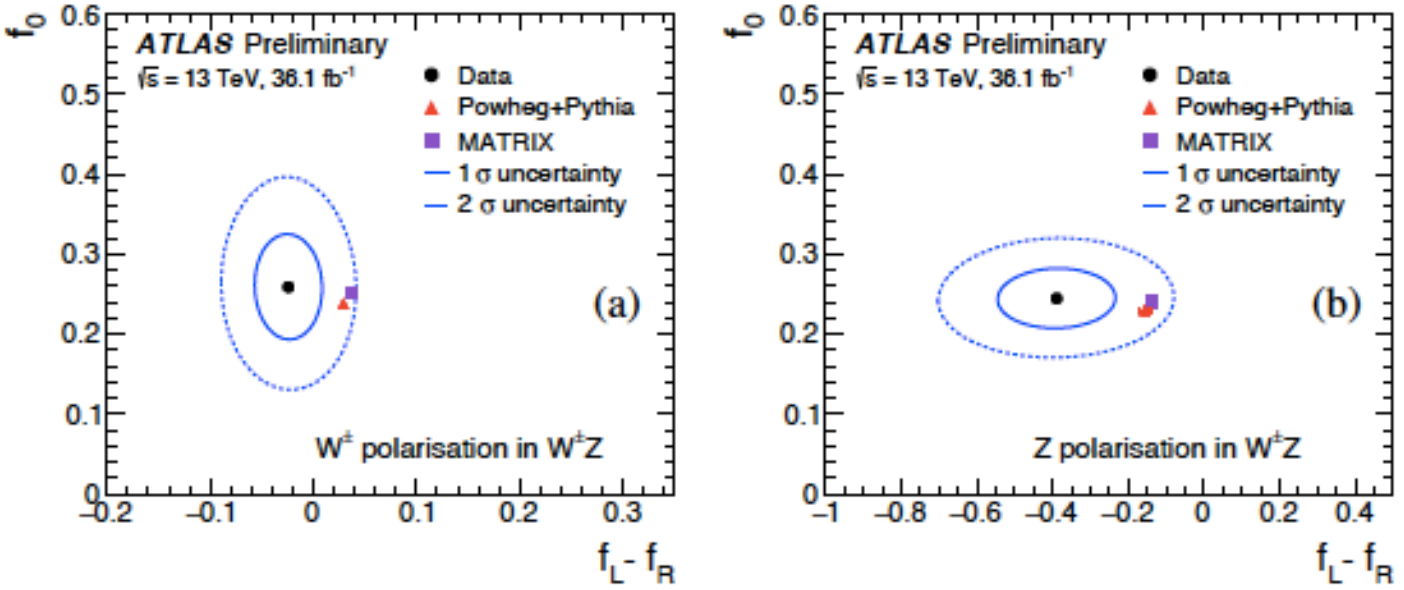

Figure 10: Measured helicity fractions f_0 and $f_L - f_R$ for the W (a) and Z (b) bosons in $W^\pm Z$ events, compared to the prediction from Powheg+Pythia (red triangle) and MATRIX (purple square). Theory uncertainties on the Powheg+Pythia prediction arising from PDF and QCD scale uncertainties are of the same size as the triangle marker. The full and dashed ellipses around the data points correspond to one and two standard deviations, respectively.

Observation of same-sign WW EW process

- Table below shows the relative importances of the different backgrounds to the same-sign WW EW process
- Dominant backgrounds are from WZjj QCD (normalised to data from three-lepton control region) and from misidentified leptons, plus, in the case of electrons, charge misid. and prompt photon conversions from Vγ processes

$W^{\pm}W^{\pm}jj$ EW

Process	Yield in signal region
$WZjj$ QCD	32 ± 9
Other prompt	2.4 ± 0.5
Prompt $V\gamma$ and charge misid.	13.4 ± 3.5
Misid. leptons	23 ± 12
$W^{\pm}W^{\pm}jj$ QCD	7.3 ± 2.5
Expected background	78 ± 15
Expected signal	40.9 ± 2.9
Data	122

Table 14: Expected background and signal yields in signal region for same-sign WW EW process.

Observation of same-sign WW VBS EW process
Fiducial cross section

- **Same-sign WW EW :** $\sigma^{\text{fid}} = 2.91^{+0.51}_{-0.47}\ (\text{stat.}) \pm 0.27\ (\text{sys.})\ \text{fb}$

- **What about predictions?**
  Same-sign WW process is the only diboson process to-date for which NLO (EW and QCD) corrections have been computed.
  B. Biedermann, A. Denner, and M. Pellen
  See also A. Ballestrero et al.

  Main impact of improved calculation arises from NLO EW corrections which are negative and correspond to ≈ -15% in the fiducial region of interest.
  σ_{LO}^{fid} = 1.64 fb with ≈ 10% uncertainty
  σ_{NLO}^{fid} = 1.36 fb with ≈ 2% uncertainty
  Overall a 20% reduction of the fiducial cross section which is unambiguous at this order only in terms of final-state leptons and partons.

  Predictions seem low (choice of scales = sqrt($p_T^{j1} \times p_T^{j2}$)? something else?)

Observation of same-sign WW VBS EW process

- **Same-sign WW :** $\sigma^{\text{fid}} = 2.91^{+0.51}_{-0.47}\ (\text{stat.}) \pm 0.27\ (\text{sys.})\ \text{fb}$

Fiducial cross sections at LO for same-sign WWjj EW process:
Sherpa v2.2.2: 2.0 ± 0.3 fb
Powheg+Pythia8: 3.1 ± 0.5 fb

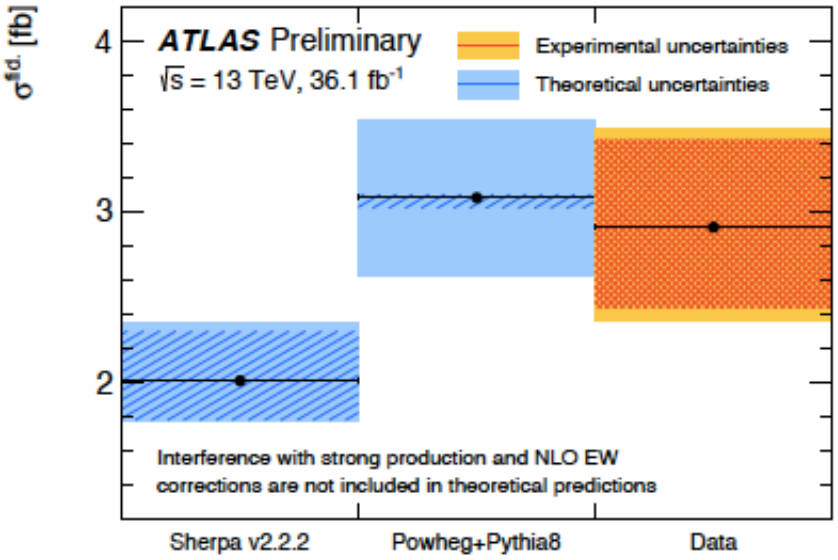

Figure 3: Comparison of the measured fiducial cross section and the theoretical calculations from SHERPA v2.2.2 and POWHEGBOX+PYTHIA8. Statistical uncertainties in the measured value are depicted as a checked orange band while the combined statistical and experimental uncertainty is shown as a light orange band. The theoretical uncertainties from the scale dependence are depicted as a dashed blue band while the total theoretical uncertainties which includes uncertainties in the PDF and parton shower model are depicted by a light blue band. The theoretical predictions include neither the interference of $W^{\pm}W^{\pm}jj$ electroweak and strong production (arXiv:1803.07943), nor the NLO electroweak corrections (JHEP **10** (2017) 124).

Measurement of $\sin^2\theta^l_{eff}$

From GFITTER 2018

Parameter	Input value	Free in fit	Fit Result	w/o exp. input in line	w/o exp. input in line, no theo. unc
M_H [GeV]$^{(\diamond)}$	125.14 ± 0.24	yes	125.14 ± 0.24	93^{+25}_{-21}	93^{+24}_{-20}
M_W [GeV]	80.385 ± 0.015	–	80.364 ± 0.007	80.358 ± 0.008	80.358 ± 0.006
Γ_W [GeV]	2.085 ± 0.042	–	2.091 ± 0.001	2.091 ± 0.001	2.091 ± 0.001
M_Z [GeV]	91.1875 ± 0.0021	yes	91.1880 ± 0.0021	91.200 ± 0.011	91.2000 ± 0.010
Γ_Z [GeV]	2.4952 ± 0.0023	–	2.4950 ± 0.0014	2.4946 ± 0.0016	2.4945 ± 0.0016
σ^0_{had} [nb]	41.540 ± 0.037	–	41.484 ± 0.015	41.475 ± 0.016	41.474 ± 0.015
R^0_ℓ	20.767 ± 0.025	–	20.743 ± 0.017	20.722 ± 0.026	20.721 ± 0.026
$A^{0,\ell}_{FB}$	0.0171 ± 0.0010	–	0.01626 ± 0.0001	0.01625 ± 0.0001	0.01625 ± 0.0001
A_ℓ $^{(*)}$	0.1499 ± 0.0018	–	0.1472 ± 0.0005	0.1472 ± 0.0005	0.1472 ± 0.0004
$\sin^2\theta^\ell_{eff}(Q_{FB})$	0.2324 ± 0.0012	–	0.23150 ± 0.00006	0.23149 ± 0.00007	0.23150 ± 0.00005

- **Recently, legacy Tevatron combination result published**
- **Very recently, CMS 8 TeV measurement published**
- **Both measurements based on fiducial A_{FB} measurements**
- **Here, show results based on a measurement of angular coefficients from Z-boson decay**

Angular coefficients A_0-A_7 and A_{FB}

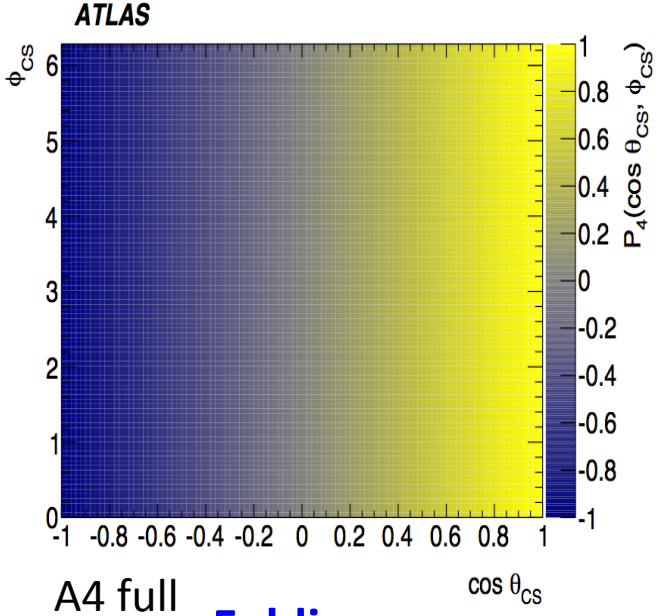

A4 full phase space

Folding

A4 fid. phase space

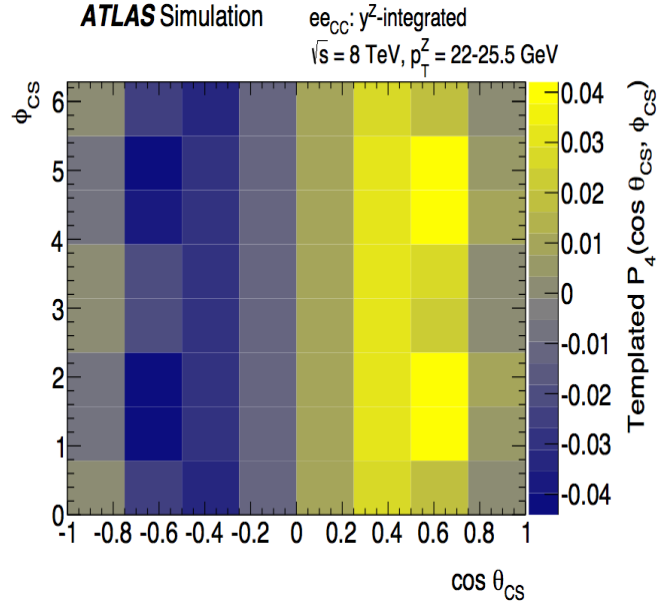

$$\frac{d^5\sigma}{dp_T^Z\, dy^Z\, dm^Z\, d\cos\theta\, d\phi} = \frac{3}{16\pi}\frac{d^3\sigma^{U+L}}{dp_T^Z\, dy^Z\, dm^Z}$$

$$\{(1+\cos^2\theta) + 1/2\, A_0(1-3\cos^2\theta) + A_1 \sin 2\theta \cos\phi$$
$$+1/2\, A_2 \sin^2\theta \cos 2\phi + A_3 \sin\theta \cos\phi + A_4 \cos\theta$$
$$+A_5 \sin^2\theta \sin 2\phi + A_6 \sin 2\theta \sin\phi + A_7 \sin\theta \sin\phi\}.$$

- **Angular coefficients encapsulate all QCD production dynamics**
- **A_{FB} = 3/8 A_4 in full phase space of decay leptons at all orders in QCD**
- **Direct measurement of angular coefficients A_4 + A_3 leads to measurement of $\sin^2\theta^l_{eff}$**
- **Based on effective linear relation:**
  $A4 = a \times \sin^2\theta^l_{eff} + b$
  predicted in each measurement bin
- **Measurement based on:**
  - **6M eeCC events ($0 < |\eta| < 2.5$)**
  - **7.5M $\mu\mu$CC events ($0 < |\eta| < 2.5$)**
  - **1.5M eeCF events**
    ($0 < |\eta| < 2.5$ and $2.5 < |\eta| < 4.9$)

Angular coefficients A_0-A_7 and A_{FB}

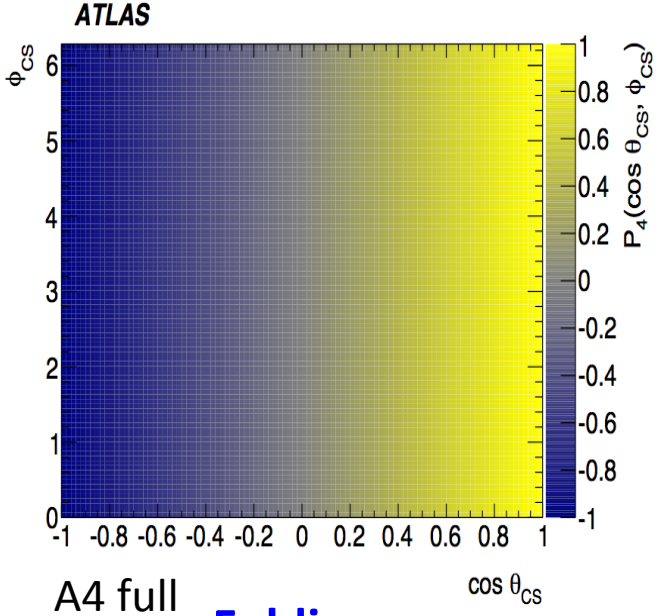

A4 full phase space

Folding

A4 fid. phase space

$$N^n_{\text{exp}}(A,\sigma,\theta) = \left\{ \sum_{j=0}^{N_{\text{bins}}} \sigma_j \times L \times \left[t^n_{8j}(\beta) + \sum_{i=0}^{7} A_{ij} \times t^n_{ij}(\beta) \right] \right\} \times \gamma^n + \sum_{B}^{\text{bkgs}} T^n_B(\beta),$$

where:

- $N_{\text{bins}} = 1280$ is the total number of measurement bins in $(\cos\theta, \phi, m^{\ell\ell}, y^{\ell\ell})$ space
- A is the set of all angular coefficients, A_{ij}
- σ is the set of all polarised cross sections, σ_j
- θ is the set of all nuisance parameters representing the systematic uncertainties, $\{\beta^m, \gamma^n\}$
- t_{ij} is the set of all signal P_i templates
- T_B is the set of background templates, where the sum runs over all background sources
- L is the total integrated luminosity.

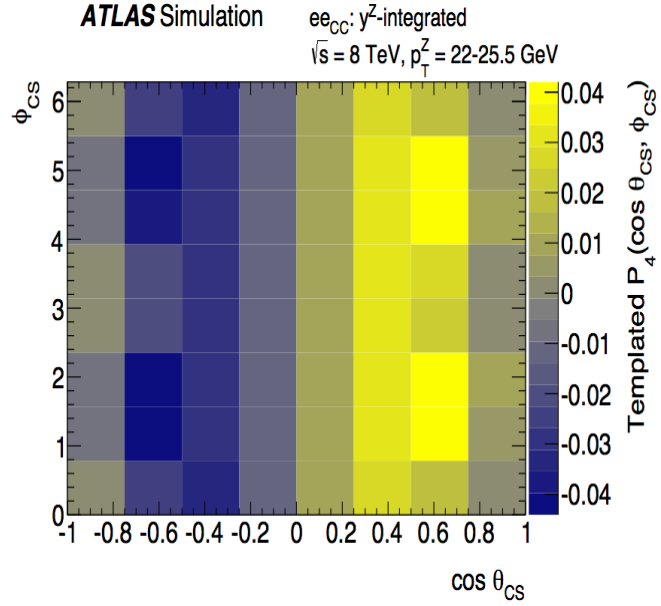

- **Technically more challenging than A_{FB}, but some advantages**
  - **Angular variables can constrain experimental systematics**
  - **Measurements in full phase space via analytical extrapolation**
    - **Reduced theory uncertainties**
    - **Can impose channel-to-channel cross-section constraint without extrapolation**
- **Possibly more sensitive to NLO EW effects that can break harmonic decomposition compared to A_{FB} (but can be accounted for with corrections)**

Measurement of $\sin^2\theta^l_{eff}$ using A_4 angular coefficient

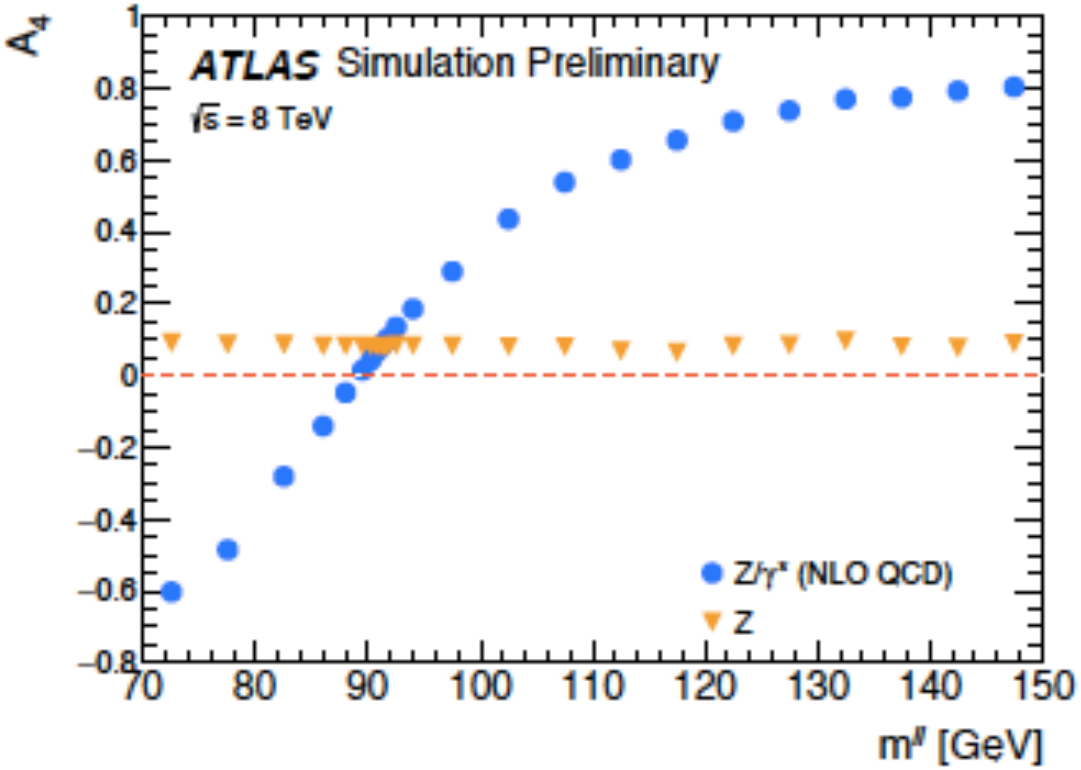

- Asymmetry (shown here for A_4) varies strongly versus m_{ll} but mostly because of Z/γ^* interference
- Asymmetry due to weak mixing angle is small and ≈ constant:
  → no need to have fine mass binning around m_Z
  → use sidebands around Z pole to constrain PDFs (see later)

A4 analysis: predictions

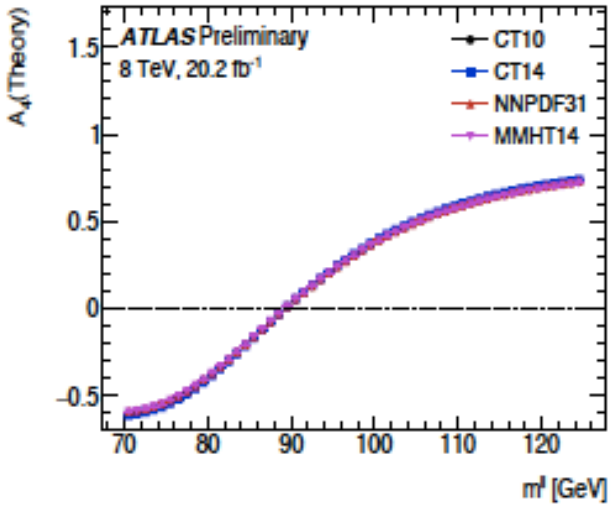

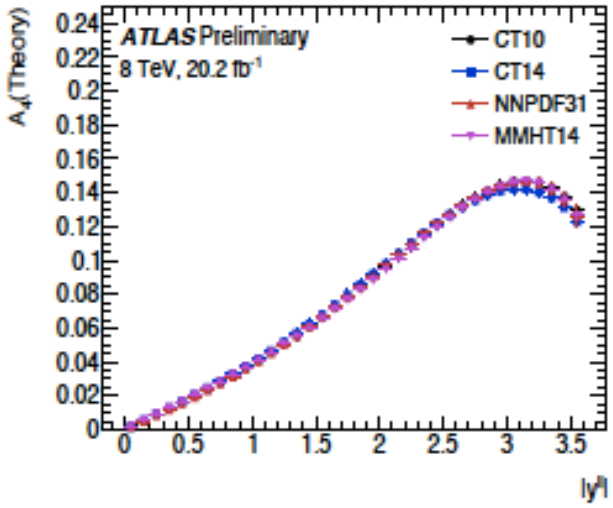

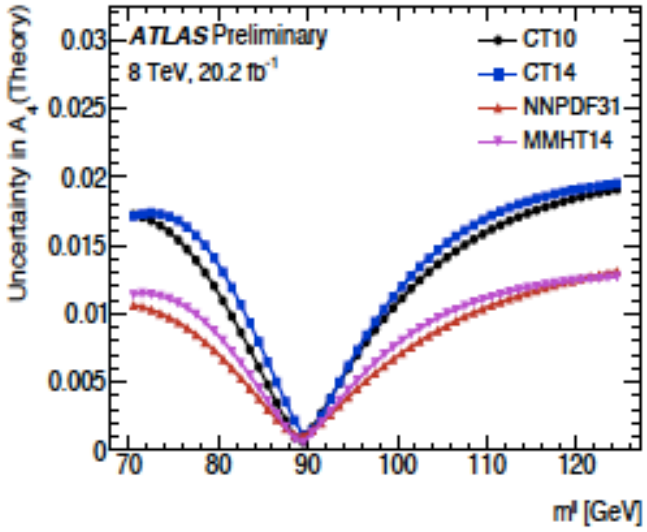

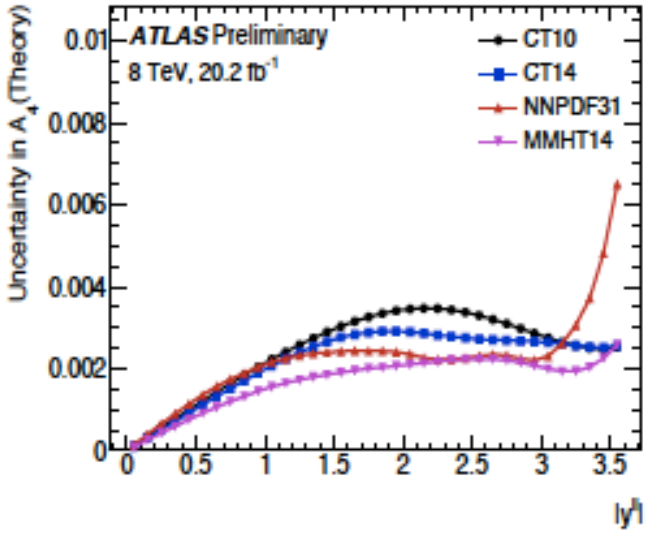

- **Fixed-order predictions of A_4 using DYTurbo (optimised version of DYRES/DYNNLO):**
  - **NLO QCD**
  - **LO EW**
  - **PDG $\sin^2\theta_W$ for central value**

A_4 largest at $y^Z \sim 3$

- **y^{ll} shape driven by dilution effects**
- **m^{ll} shape driven by Z/γ^* interference**

Uncertainty on A_4 largest above and below the mass pole

- **Can be used to profile PDFs**

EW corrections, improved Born approximation, and definition of $\sin^2\theta^{\ell}_{\text{eff}}$

The EW virtual corrections can be expressed fully in terms of several complex form factors, which account for the higher-order virtual corrections, including those to the photon and Z-boson propagators. The flavour-dependent EW form factors $K_f(s,t)$ modify directly the vector couplings of the Z boson to fermions as follows:

$$v_f = (2 \cdot T_3^f - 4 \cdot q_f \cdot \sin^2\theta_W \cdot K_f(s,t))/\Delta, \quad (3)$$

where (s,t) denote two variables, chosen to be $m^{\ell\ell}$ and $\cos\theta$ (the dependence on the lepton angular variable arises from the inclusion of box corrections), T_3^f represents the third component of the fermion weak isospin and q_f the fermion electric charge, the parameter $\sin^2\theta_W = 1 - m_W^2/m_Z^2$ is the weak mixing angle in the on-mass-shell scheme, and $\Delta = \sqrt{16 \cdot \sin^2\theta_W \cdot (1 - \sin^2\theta_W)}$ is a multiplicative factor. At the Z pole, if one integrates over t and considers Z-boson decays to leptons ignoring the small contribution from the imaginary part of K_f, the ratio of the effective vector to axial-vector coupling constants of the Z boson to leptons is expressed as a function of a single effective form factor K_Z^{ℓ}:

$$\frac{v_l}{a_l} = 1 - 4 \cdot K_Z^{\ell} \cdot \sin^2\theta_W, \quad (4)$$

and one can define the effective leptonic weak mixing angle at the Z pole as: $\sin^2\theta_{\text{eff}}^{\ell} = K_Z^{\ell} \cdot \sin^2\theta_W$.

EW corrections using improved Born approximation (IBA)

$$wt^{EW} = \frac{d\sigma_{Born+EW}(x_1, x_2, \hat{s}, \cos\theta^*, s_W^2)}{d\sigma_{Born}(x_1, x_2, \hat{s}, \cos\theta^*, s_W^2)}$$

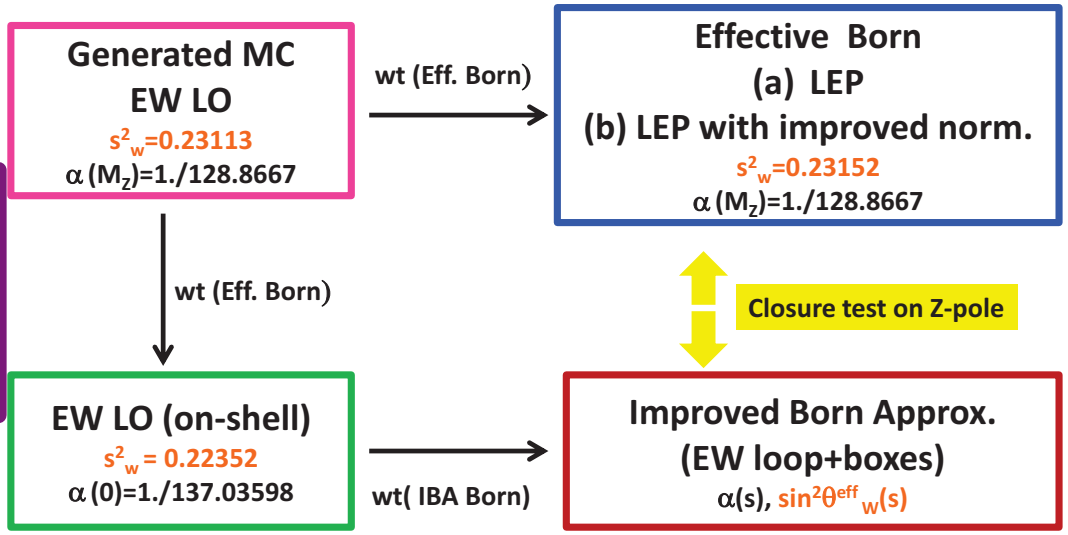

- The most precise calculations available today still come from LEP1 legacy code (D. Bardin et al., Dizet library 6.21) and IBA approach extended from lepton colliders to hadron colliders (Mustraal reference frame, extended to W boson, and validated for EW weight averaged over incoming u/d partons)
- Most MC tools today are LO EW and use PDG value or similar for $\sin^2\theta_W$
- Define per-event weight to apply EW corrections to Z couplings and to γ^* and Z propagators for any MC sample, based on LO EW in any scheme
- This IBA from LEP1 legacy code corresponds to specific EW scheme ($\alpha(0)$, m_z, G_μ) chosen for best matching to knowledge at the time and to LEP measurements sensitive to $\sin^2\theta^{l}_{eff}$

EW corrections using improved Born approximation (IBA)

Parameter	Value	Description
	Measured	
m_Z	91.1876 GeV	Mass of Z boson
m_H	125.0 GeV	Mass of Higgs boson
m_t	173.0 GeV	Mass of top quark
m_b	4.7 GeV	Mass of b quark
$1/\alpha(0)$	137.0359895(61)	QED coupling constant in Thomson limit
G_μ	$1.166389(22) \cdot 10^{-5}$ GeV^{-2}	Fermi constant from muon lifetime
	Calculated	
m_W	80.353 GeV	Mass of W boson
$\sin^2\theta_W$	0.22351946	On mass-shell-value of weak mixing angle
$\alpha(m_Z^2)$	0.00775995	
$1/\alpha(m_Z^2)$	128.86674175	
$ZPAR(6) - ZPAR(8)$	0.23175990	$sin^2\theta^\ell_{eff}(m_Z^2)$ (e, μ, τ)
$ZPAR(9)$	0.23164930	$sin^2\theta^u_{eff}(m_Z^2)$ (up quark)
$ZPAR(10)$	0.23152214	$sin^2\theta^d_{eff}(m_Z^2)$ (down quark)

Table 1: Input parameters used by the `Dizet 6.21` library together with the calculated results for effective weak mixing angles and $\alpha(m_Z)$ at the Z pole.

- **Input parameters (from measurements) of Dizet library and calculated flavour-dependent effective mixing angles**
- **Note that with today's best knowledge, $\sin^2\theta^l_{eff}$ is predicted as 0.23176 (not 0.23152)**

A4 analysis: predictions

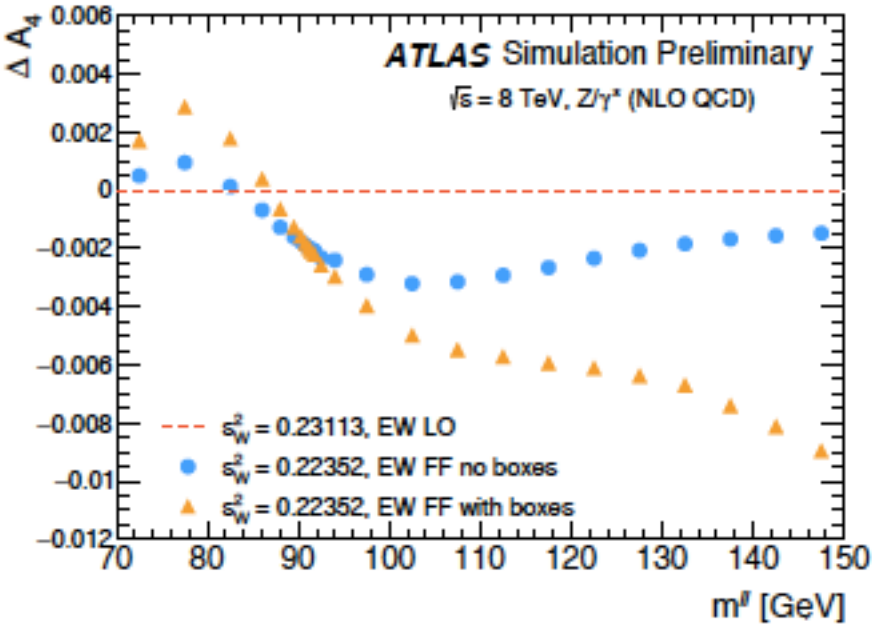

- Impact of EW form factor (FF) corrections compared to Powheg LO EW reference for predicted A4 in two cases:
  - no box diagrams included
  - with box diagrams included

  Box diagrams potentially break factorisation assumption which is at the root of angular coefficient formalism
- Impact is small near Z pole, much larger as one approaches $m^{ll} = 2m_W$

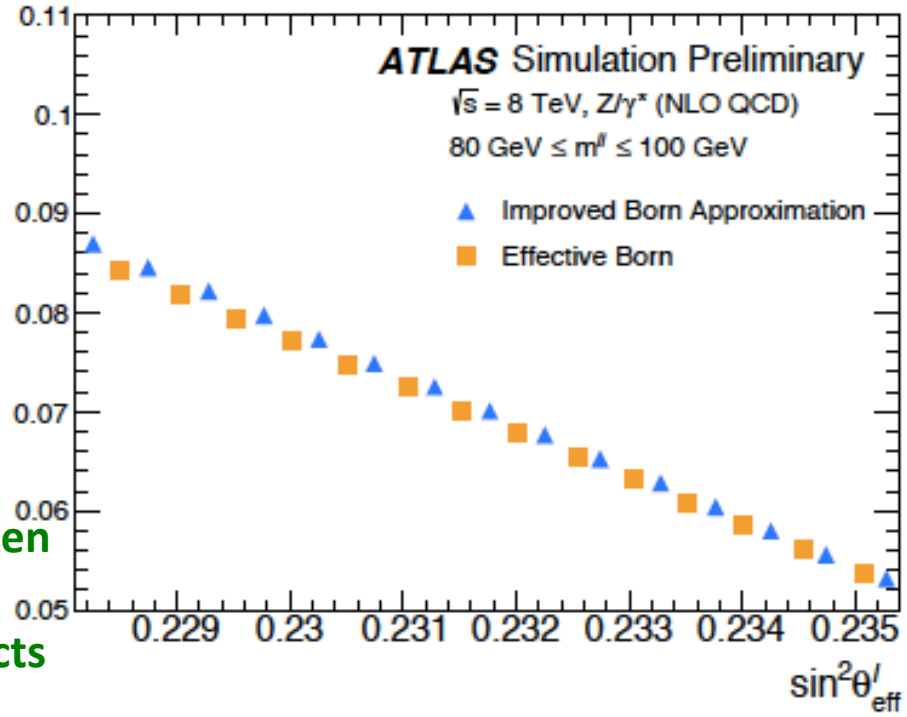

- Predicted A4 versus $\sin^2\theta^l_{eff}$
- Variations of $\sin^2\theta^l_{eff}$ implemented as small variations of vector coupling of Z boson around reference PDG value (0.23152)
- Other possible variations, eg Gm or mtop, (if performed consistently!) lead to similar results within $3\ 10^{-5}$
- Overall uncertainty on EW corrections is taken to be $3\ 10^{-5}$, including parametric uncertainties and small residual IFI/ISR effects

A4 predictions (NNLO QCD + EW corrections)

	$70 < m^{\ell\ell} < 80$ GeV			$80 < m^{\ell\ell} < 100$ GeV				$100 < m^{\ell\ell} < 125$ GeV		
$\lvert y^{\ell\ell}\rvert$	0 – 0.8	0.8 – 1.6	1.6 – 2.5	0 – 0.8	0.8 – 1.6	1.6 – 2.5	2.5 – 3.6	0 – 0.8	0.8 – 1.6	1.6 – 2.5
Central value (NNLO QCD)	−0.0870	−0.2907	−0.5970	0.0144	0.0471	0.0928	0.1464	0.1045	0.3444	0.6807
ΔA_4 (NNLO - NLO QCD)	0.0003	0.0010	0.0021	−0.0001	−0.0005	−0.0009	−0.0015	−0.0007	−0.0022	−0.0041
ΔA_4 (EW)	0.0008	0.0028	0.0056	0.0002	0.0007	0.0015	0.0026	−0.0008	−0.0026	−0.0048
$\Delta \sin^2\theta^{\ell}_{\text{eff}}$ (EW)	0.00129	0.00130	0.00133	0.00024	0.00024	0.00025	0.00026	−0.00120	−0.00123	−0.00119
	Uncertainties			Uncertainties				Uncertainties		
Total	0.0035	0.0094	0.0137	0.0007	0.0017	0.0021	0.0021	0.0040	0.0102	0.0140
PDF	0.0034	0.0092	0.0127	0.0007	0.0016	0.0020	0.0019	0.0039	0.0100	0.0131
QCD scales	0.0006	0.0019	0.0052	0.0003	0.0003	0.0004	0.0008	0.0005	0.0022	0.0049

Table 2: Predicted values of A_4 at NNLO in QCD for the ten measurement bins in $(m^{\ell\ell}, |y^{\ell\ell}|)$ space, together with their uncertainties from PDFs, as obtained from the MMHT14 PDF set, and from factorisation and renormalisation scale variations, as obtained from the NLO predictions. The impact, ΔA_4 (NNLO - NLO QCD), of moving from NLO to NNLO QCD predictions is shown for each measurement bin. The predictions include the EW form factor corrections discussed in the text. The impact, ΔA_4 (EW), in each bin of these corrections on the predictions is also shown, as well as the impact, $\Delta \sin^2\theta^{\ell}_{\text{eff}}$ (EW), on the value of $\sin^2\theta^{\ell}_{\text{eff}}$ inferred from the predicted A_4.

- **Predictions obtained at NNLO in QCD (fixed order) and EW corrections implemented using EW weights and IBA.**
- **PDF uncertainties dominate predictions, even using NLO QCD scale variations**
- **Predict A4 = a * + b $\sin^2\theta^{l}_{\text{eff}}$ in each bin, where EW corrections are absorbed in (a,b)**
- **Impact of EW corrections ≈ 24 10^{-5} in pole region compared to LO EW MC with $\sin^2\theta_W = 0.23152$ (these are averaged over each (m^{ll}, $|y^{ll}|$) bin**

Data analysis

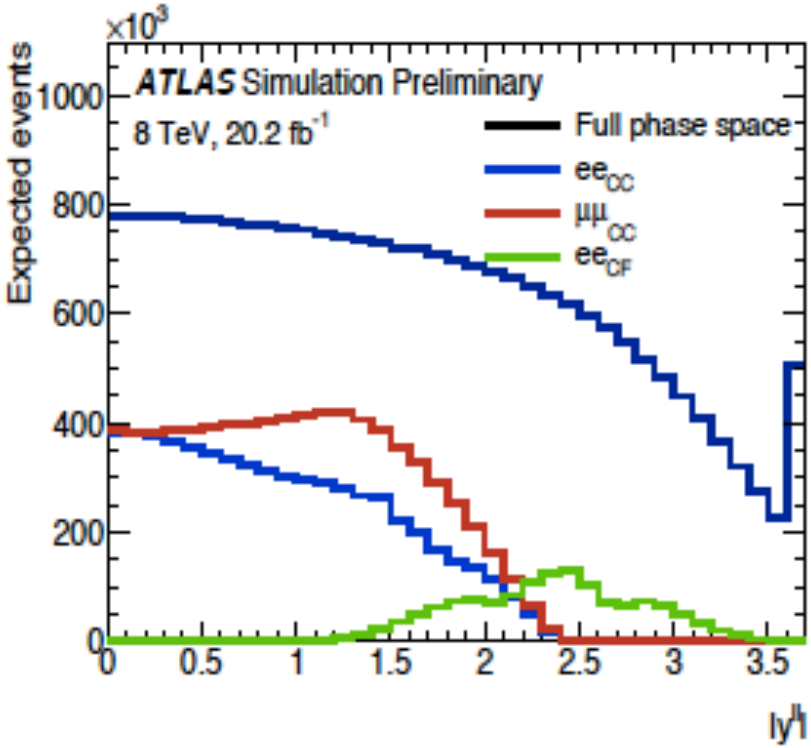

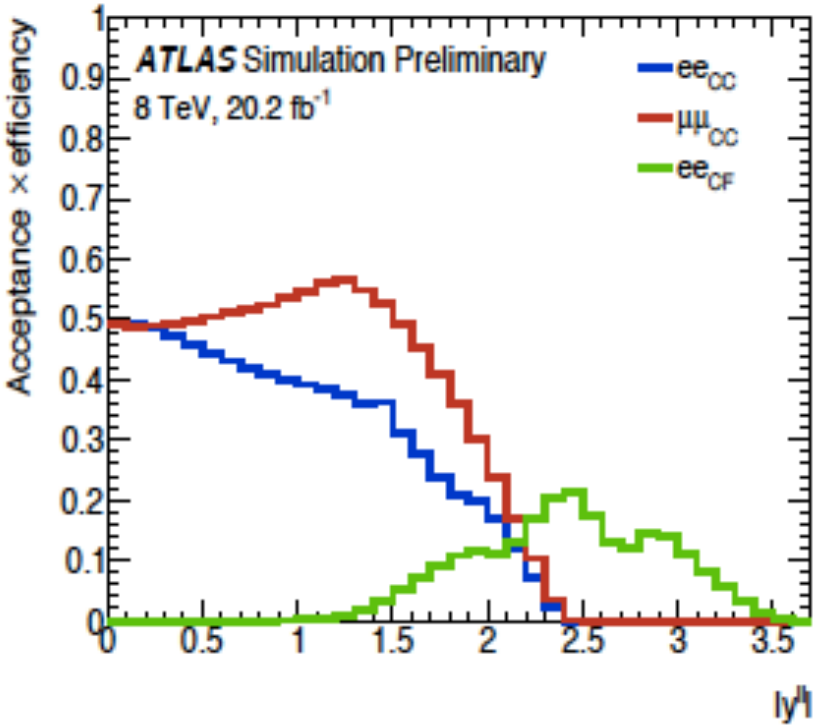

- **Expected event yields and products of acceptance and selection efficiencies for different analysis channels**

Data analysis: eeCC channel

	$70 < m_{ll} < 80$ GeV			
$\lvert y_{ll}\rvert$	Data	Top+EW	Multijets	Non-fiducial Z
0-0.8	106 718	0.023	0.015	0.010
0.8-1.6	95 814	0.015	0.020	0.010
1.6-2.5	47 078	0.012	0.041	0.009
	$80 < m_{ll} < 100$ GeV			
$\lvert y_{ll}\rvert$	Data	Top+EW	Multijets	Non-fiducial Z
0-0.8	2 697 316	0.003	0.001	< 0.001
0.8-1.6	2 084 856	0.002	0.001	< 0.001
1.6-2.5	839 424	0.002	0.002	< 0.001
	$100 < m_{ll} < 125$ GeV			
$\lvert y_{ll}\rvert$	Data	Top+EW	Multijets	Non-fiducial Z
0-0.8	106 855	0.034	0.016	0.023
0.8-1.6	80 403	0.025	0.019	0.027
1.6-2.5	28 805	0.015	0.025	0.029

Expected event yields and backgrounds for eeCC channel

Data analysis: eeCC channel

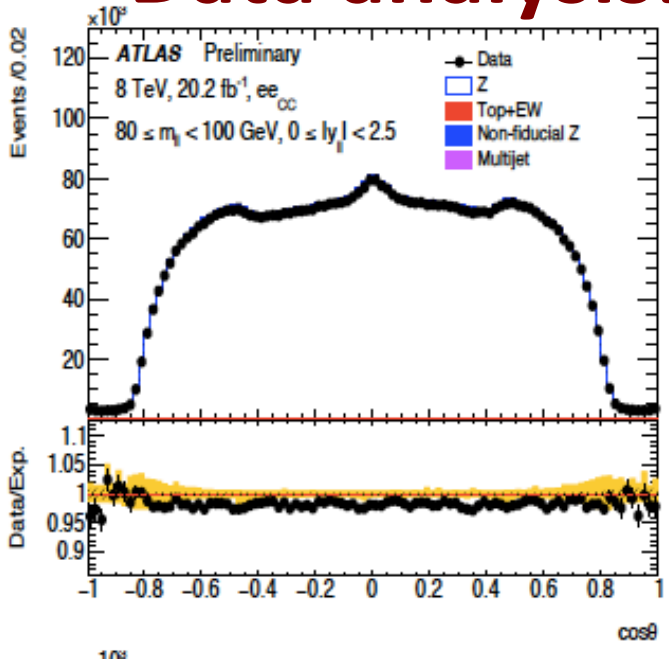

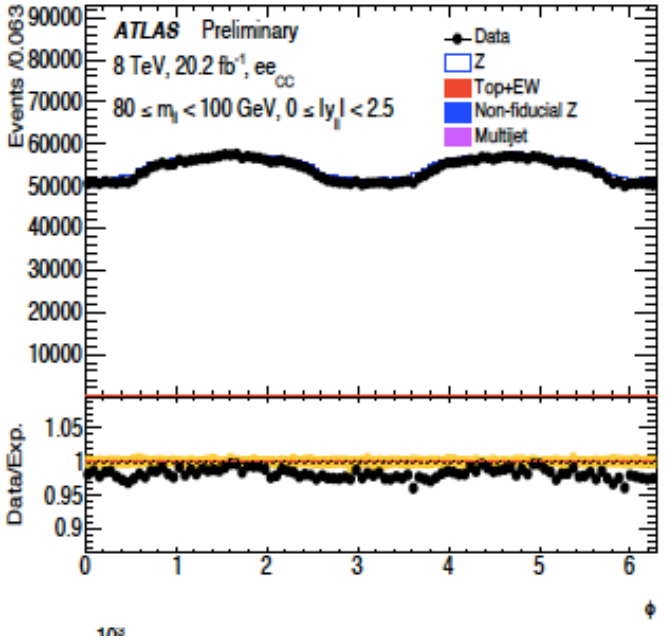

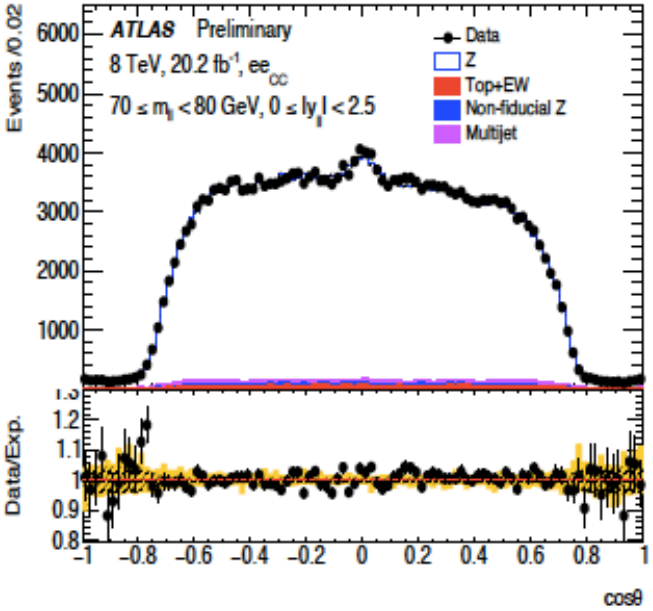

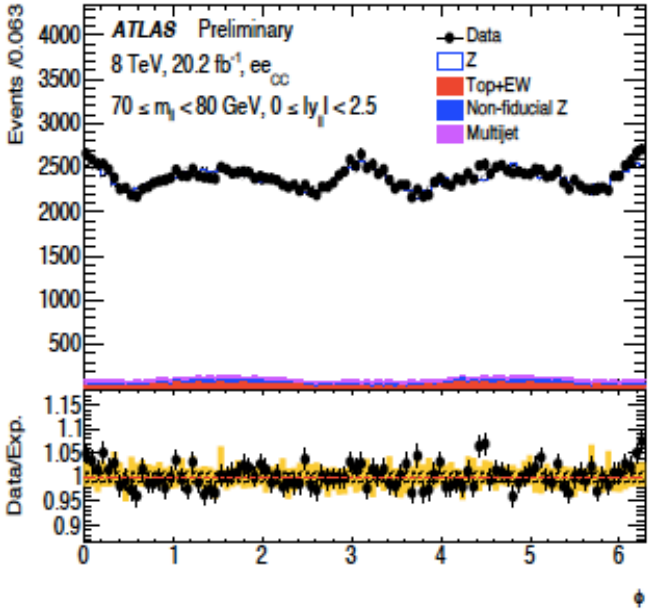

Data analysis: μμCC channel

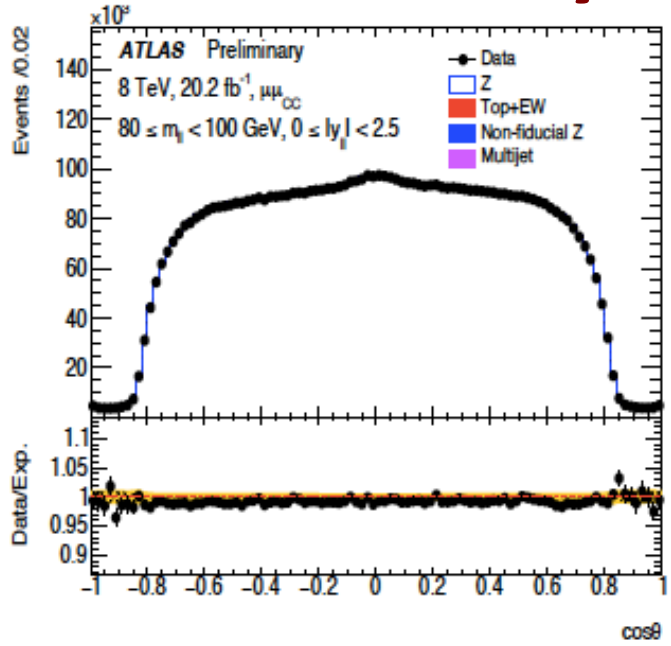

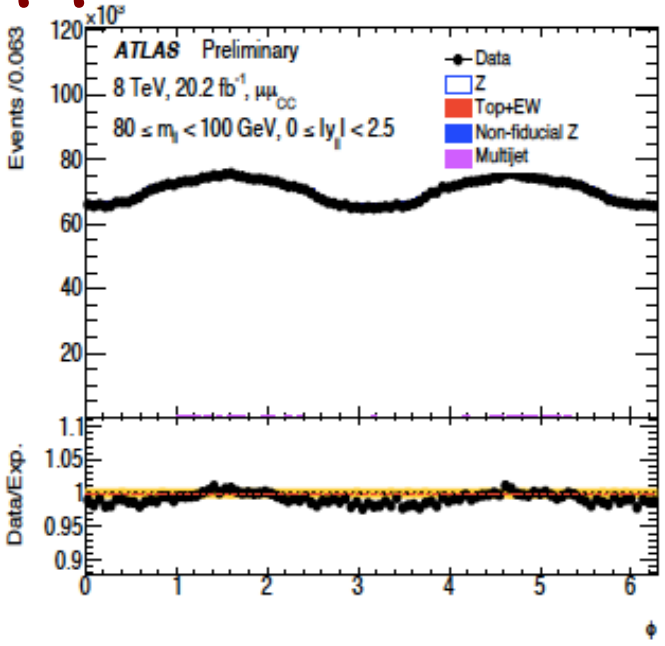

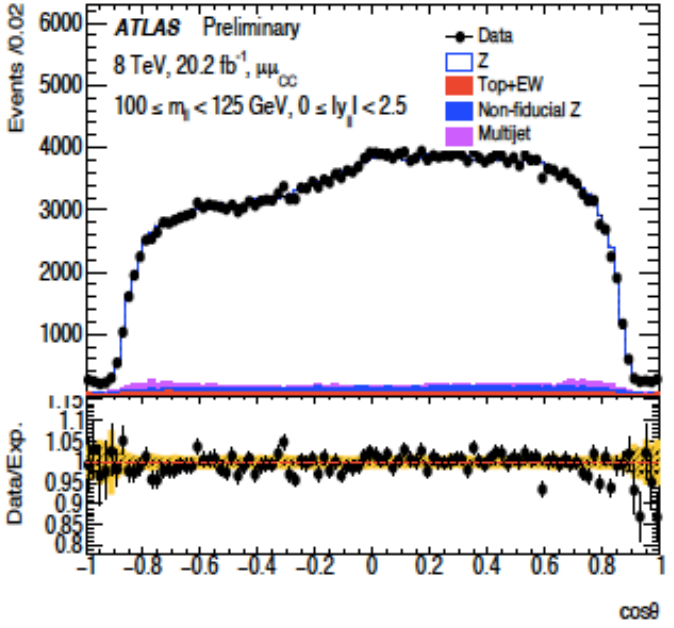

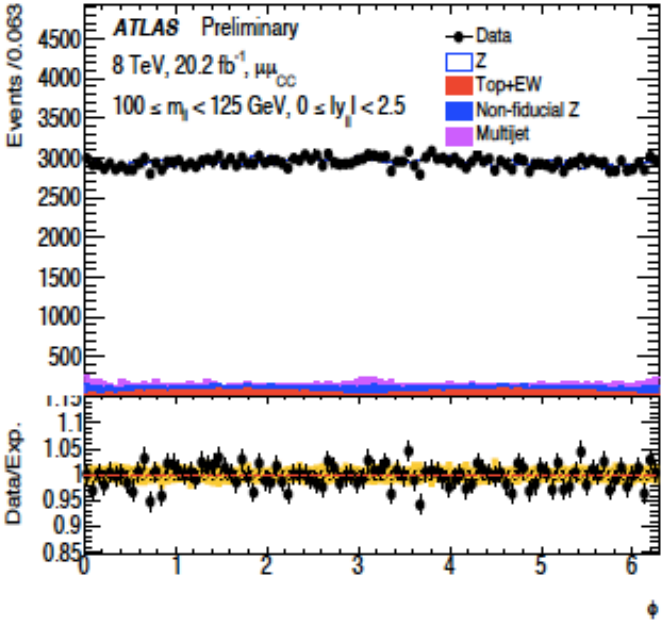

Data analysis: eeCF channel

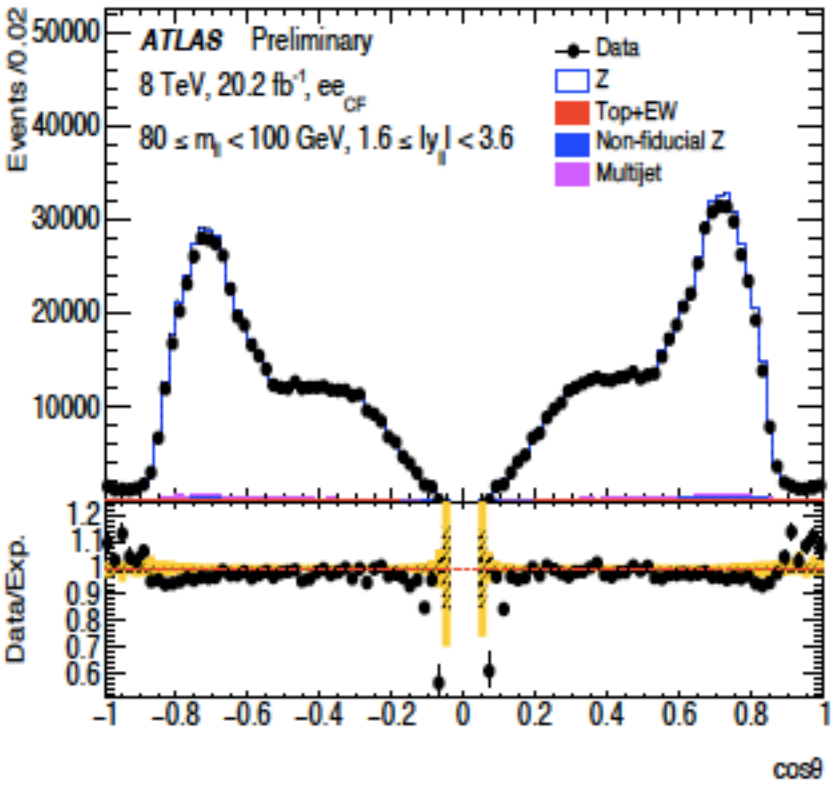

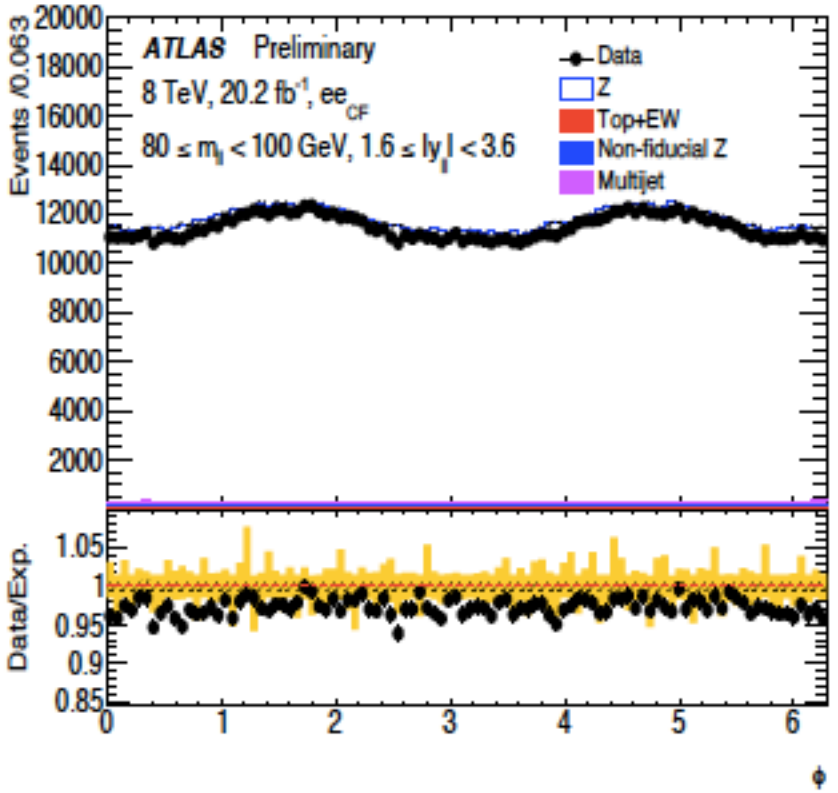

	$80 < m_{ll} < 100$ GeV			
$\lvert y_{ll}\rvert$	Data	Top+EW	Multijets	Non-fiducial Z
1.6-2.5	702 142	0.001	0.010	0.017
2.5-3.6	441 104	0.001	0.011	0.013

Expected event yields and backgrounds for different eeCF channel

A4 analysis: measurement of A4 (expected)

$m^{\ell\ell}$ (GeV)	80 – 100			
$\|y^{\ell\ell}\|$	0 – 0.8	0.8 – 1.6	1.6 – 2.5	2.5 – 3.6
Prediction (MMHT14)	0.0144	0.0471	0.0928	0.1464
	Uncertainties			
Total	0.0015	0.0015	0.0025	0.0044
Stat.	0.0013	0.0013	0.0021	0.0036
Syst.	0.0007	0.0008	0.0013	0.0025
PDF (meas.)	0.0001	0.0002	0.0004	0.0007
p_{T}^{Z} modelling	< 0.0001	< 0.0001	< 0.0001	< 0.0001
Leptons	0.0002	0.0001	0.0003	0.0007
Background	< 0.0001	< 0.0001	< 0.0001	0.0001
MC stat.	0.0007	0.0007	0.0012	0.0023

- **Expected uncertainties on measured observable A4 in pole region**
- **Results very similar to published Ai paper**
- **Stat uncertainties dominant (data and MC!)**
- **Residual PDF uncertainties an order of magnitude smaller.**
  Decorrelated from PDF uncertainties in predictions which are dominant

A4 analysis: measurement of $\sin^2\theta^l_{eff}$ (expected)

Channel	ee_{CC}	$\mu\mu_{CC}$	ee_{CF}	$ee_{CC} + \mu\mu_{CC}$	$ee_{CC} + \mu\mu_{CC} + ee_{CF}$
Total	65	59	42	48	34
Stat.	47	39	29	30	21
Syst.	45	44	31	37	27
	Uncertainties in measurements				
PDF (meas.)	7	7	7	7	4
p_T^Z modelling	< 1	< 1	1	< 1	< 1
Lepton scale	5	4	6	3	3
Lepton resolution	3	1	3	1	2
Lepton efficiency	1	1	1	1	1
Electron charge misidentification	< 1	0	< 1	< 1	< 1
Muon sagitta bias	0	4	0	2	1
Background	1	1	1	1	1
MC. stat.	25	22	18	16	12
	Uncertainties in predictions				
PDF (predictions)	36	37	21	32	22
QCD scales	5	5	9	4	6
EW corrections	3	3	3	3	3

- **Expected uncertainties on $\sin^2\theta^l_{eff}$**
- **Stat uncertainty on eeCF smaller than combined eeCC+μμCC!**
- **Dominant syst. uncertainty from PDFs: 20 10^{-5} after profiling**
- **Next dominant uncertainty from MC stats: 12 10^{-5}**

A4 measurements: compatibility tests with data

	$70 < m^{\ell\ell} < 80$ GeV			$80 < m^{\ell\ell} < 100$ GeV			$100 < m^{\ell\ell} < 125$ GeV		
$\lvert y^{\ell\ell}\rvert$	0 – 0.8	0.8 – 1.6	1.6 – 2.5	0 – 0.8	0.8 – 1.6	1.6 – 2.5	0 – 0.8	0.8 – 1.6	1.6 – 2.5
ΔA_4	0.012	0.067	0.065	−0.003	−0.001	−0.006	0.011	0.013	−0.086
	Uncertainties			Uncertainties			Uncertainties		
Total	0.034	0.039	0.078	0.003	0.003	0.007	0.017	0.019	0.045
Stat.	0.030	0.034	0.067	0.003	0.003	0.006	0.015	0.016	0.038
Syst.	0.017	0.021	0.040	0.001	0.001	0.003	0.008	0.010	0.024
PDF (meas.)	0.001	0.003	0.005	< 0.001	< 0.001	< 0.001	0.001	0.001	0.001
Leptons	0.005	0.010	0.016	< 0.001	< 0.001	< 0.001	0.002	0.007	0.012
Background	0.001	0.002	0.005	< 0.001	< 0.001	< 0.001	< 0.001	< 0.001	0.004
MC stat.	0.016	0.018	0.036	0.001	0.001	0.003	0.008	0.008	0.020

Table 9: Differences in the measured A_4 values, $\Delta A_4 = A_4(ee_{CC}) - A_4(\mu\mu_{CC})$, between the central-central electron and muon channels in all analysis bins, along with their breakdown of uncertainties. The uncertainty from the modelling of p_{T}^{Z} is only applied to the ee_{CF} channel and is not relevant here.

- **All A4 measurement bins compared in terms of their compatibility between eeCC and μμCC channels**
- **Results satisfactory for all channels, p-value is 34%**
- **For eeCF, only one overlapping bin with CC channels ($1.6 < |y|^{ll} < 2.5$) compatibility tested to be -0.0007 ± 0.0051**

A4 analysis: compatibility tests with data

Tested difference	$ee_{CC} - \mu\mu_{CC}$	$ee_{CC} - ee_{CF}$	$\mu\mu_{CC} - ee_{CF}$	$ee_{CF} - (ee_{CC} + \mu\mu_{CC})$
$\Delta \sin^2 \theta^{\ell}_{\text{eff}}$	44	−7	−51	−32
	Uncertainties			
Total	72	70	64	57
Stat.	62	56	50	42
Syst.	37	41	40	38

Table 10: Differences in the measured values of $\sin^2 \theta^{\ell}_{\text{eff}}$, $\Delta \sin^2 \theta^{\ell}_{\text{eff}}$, between the various channels, along with their global breakdown of uncertainties. The values are shown in units of 10^{-5}.

- **All channels compared in terms of their compatibility for $\sin^2\theta^{l}_{\text{eff}}$**
- **Results satisfactory for all channels**
- **Most stringent test for last column:**
  still, test at the level of ≈ 50 10^{-5} sensitivity compared to 30 10^{-5} expected sensitivity of the final measurement.

A4 analysis: compatibility tests with data

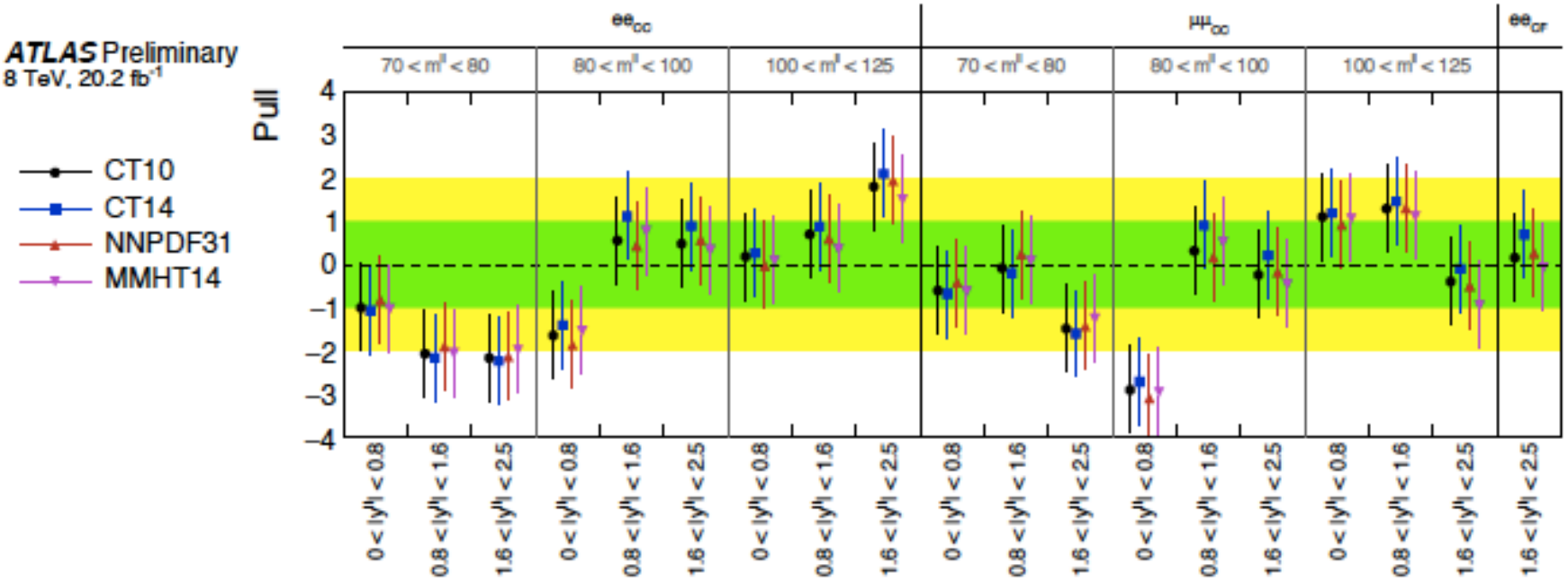

Figure 8: For 19 out of 20 measurement bins over the three analysis channels, distribution of the pulls of each measurement of $\sin^2\theta^{\ell}_{\text{eff}}$ with respect to a reference chosen to be the most sensitive measurement, namely that from the ee_{CF} channel in the measurement bin $2.5 < |y^{\ell\ell}| < 3.6$. The results are shown separately for the four different PDF sets considered in this note.

- **Finally, test compatibility of all measurement bins (19 plus one reference one) as individual measurements of $\sin^2\theta^{l}_{\text{eff}}$**
- **Overall p-value only 3.4% (3s pull from low y^{ll} μμCC channel)**

$\sin^2\theta^l_{eff}$ results based on reference PDF set (MMHT14)

Channel	ee_{CC}	$\mu\mu_{CC}$	ee_{CF}	$ee_{CC} + \mu\mu_{CC}$	$ee_{CC} + \mu\mu_{CC} + ee_{CF}$
Central value	0.23148	0.23123	0.23166	0.23119	0.23140
	Uncertainties				
Total	68	59	43	49	36
Stat.	48	40	29	31	21
Syst.	48	44	32	38	29
	Uncertainties in measurements				
PDF (meas.)	8	9	7	6	4
p_T^Z modelling	0	0	7	0	5
Lepton scale	4	4	4	4	3
Lepton resolution	6	1	2	2	1
Lepton efficiency	11	3	3	2	4
Electron charge misidentification	2	0	1	1	< 1
Muon sagitta bias	0	5	0	1	2
Background	1	2	1	1	2
MC. stat.	25	22	18	16	12
	Uncertainties in predictions				
PDF (predictions)	37	35	22	33	24
QCD scales	6	8	9	5	6
EW corrections	3	3	3	3	3

- **Fit using MMHT14 provides best overall result, i.e. best fit χ^2 and also smallest uncertainties from PDFs after profiling**

$\sin^2\theta^{l}_{eff}$ results based on reference PDF set (MMHT14)

	CT10	CT14	MMHT14	NNPDF31
$\sin^2\theta^{\ell}_{\rm eff}$	0.23118	0.23141	0.23140	0.23146
	Uncertainties in measurements			
Total	39	37	36	38
Stat.	21	21	21	21
Syst.	32	31	29	31

Table 13: Results for extracted values of $\sin^2\theta^{\ell}_{\rm eff}$ with the global breakdown of their uncertainties, shown for the four PDF sets considered in this note. The uncertainty values are given in units of 10^{-5}.

- **Fit using MMHT14 provides best overall result, i.e. best fit χ^2 and also smallest uncertainties from PDFs after profiling**
- **Results quite close for CT14 and NNPDF31, uncertainties a bit larger.**
- **CT10nnlo also shown since it fits best the ensemble of ATLAS W/Z precision data at 7 TeV used for measurement of m_W.**
- **Overall $\sin^2\theta^{l}_{eff}$ range spanned by all PDF sets is 28 10^{-5}**
- **Will discuss this further with PDF4LHC forum (see later slide)**

$\sin^2\theta^{\ell}_{\text{eff}}$ results compared to previous measurements

$$\sin^2\theta^{\ell}_{\text{eff}} = 0.23140 \pm 0.00021\,(\text{stat.}) \pm 0.00024\,(\text{PDF}) \pm 0.00016\,(\text{syst.})$$

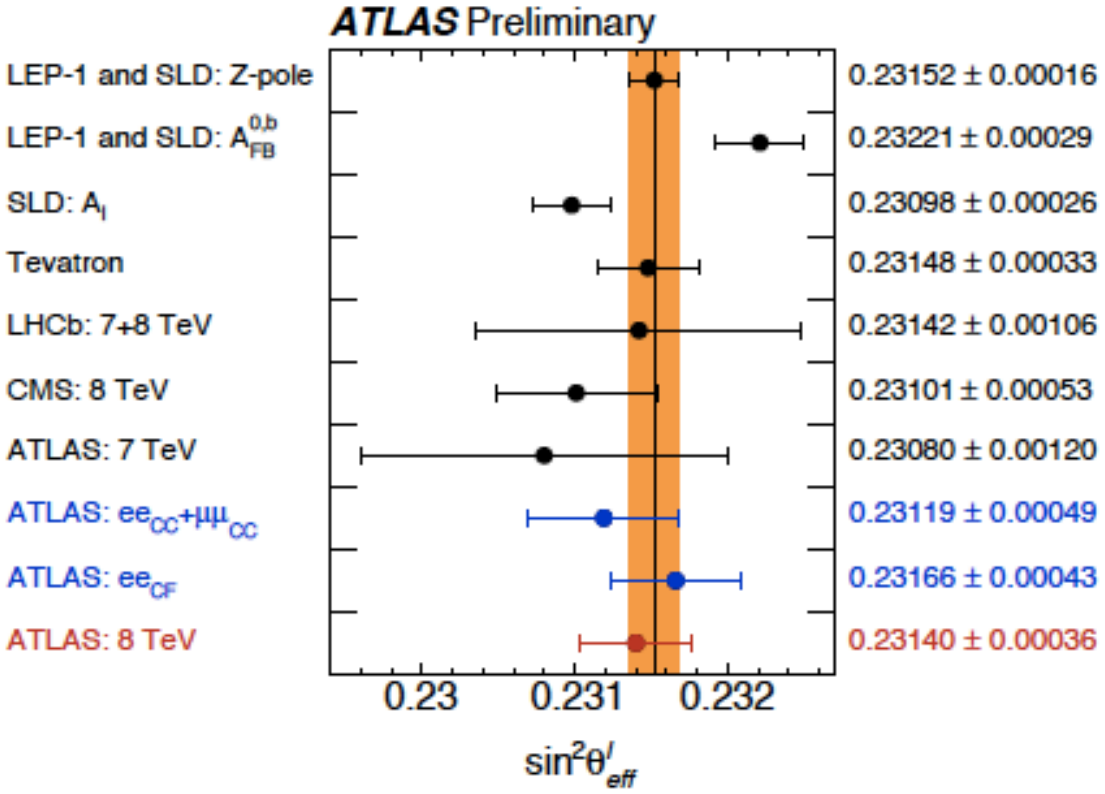

Figure 11: Comparison of the measurements of the effective leptonic weak mixing angle, $\sin^2\theta^{\ell}_{\text{eff}}$, presented in this note to previous measurements at LEP/SLC, at the Tevatron, and at the LHC. The overall LEP-1/SLD average [49] is represented together with its uncertainty as a vertical band. The ATLAS combined result for all channels is shown, together with the results for the ee_{CF} channel alone and for the combined ee_{CC} and $\mu\mu_{CC}$ channels. This latter result can be compared directly with the CMS result on the same dataset and has a similar overall accuracy.

Future prospects for $\sin^2\theta^l_{eff}$

- The hadron collider measurements of $\sin^2\theta^l_{eff}$ provide consistency tests of the SM which are now relevant on a global level, but they do rely on the SM even more than the LEP/SLC measurements did
- They will already be largely dominated by PDF uncertainties if one considers the future run-2 legacy measurements.
- Before pursuing further measurements of this type at 13 TeV with much higher stats but increased dilution, need to assess PDF uncertainties with a view focused only on precision DY measurements
- This work has begun within the context of LPCC SM precision EW working group, please join if you are interested in contributing!
  Conveners: A. Apyan, O. Lupton, F. Piccinini, M. Schmitt, T. Shears, D.F.
- Next steps of the working group:
  - Combination of LHC experiments (ATLAS, CMS and LHCb) for $\sin^2\theta^l_{eff}$
  - Combination of m_W (ATLAS and Tevatron)
  - Precise comparisons of IBA approach to other calculations (NLO EW and beyond), eg Powheg EW
  - Improved fixed-order and resummed calculations of W/Z-boson p_T spectra

Historical perspective: the 80's in UA1/UA2 at the SppS

To the end, with first accurate measurements of the W/Z masses and the search for the top quark and for supersymmetry

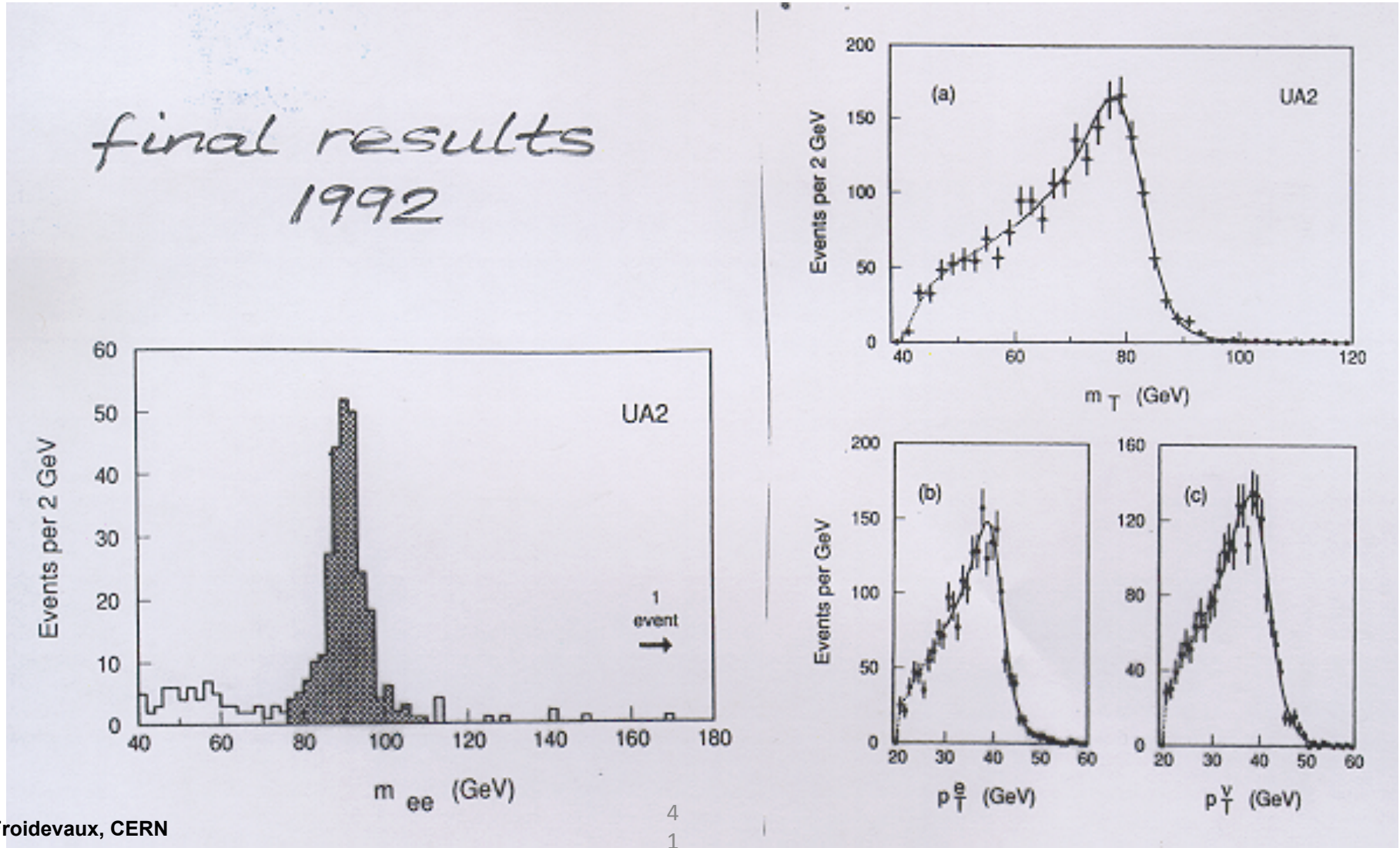

Historical perspective: the 80's in UA1/UA2 at the SppS

Most important results from 1987-1990 campaign with UA2:

precise measurement of m_W/m_Z

and direct limit on top-quark mass ($m_{top} < 60$ GeV)

Transverse mass distribution for electron-neutrino pairs

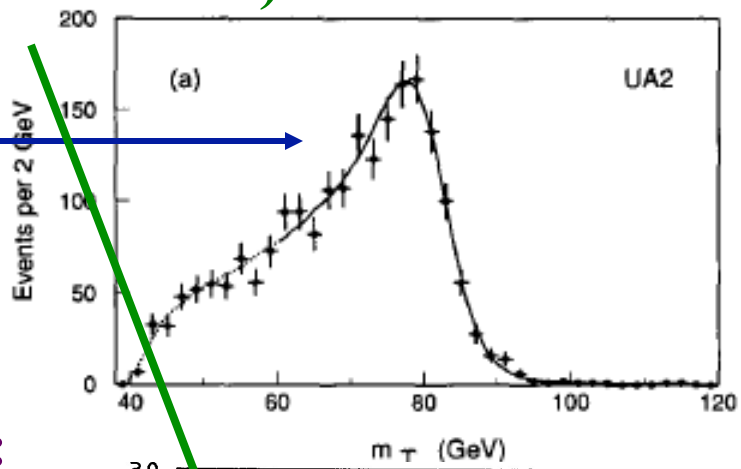

$$\frac{m_W}{m_Z} = 0.8813 \pm 0.0036 \pm 0.0019$$

Using the precise measurement of m_Z (LEP):

$$m_W = 80.35 \pm 0.33 \pm 0.17 \text{ GeV}$$

→ **Indirect limits on top-quark mass in the context of the Standard Model:**

$$m_{top} = 160^{+50}_{-60} \text{ GeV}$$

(four years before the discovery of the top quark at Fermilab)

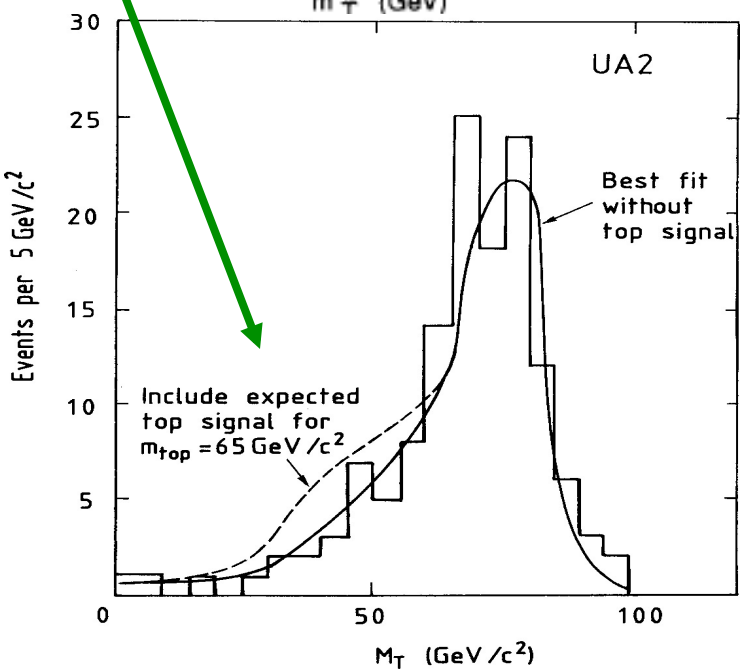

Historical perspective: the 80's in UA1/UA2 at the SppS

First ever EW fits in UA2 before LEP turned on

From these events we measure the mass of the Z^0 boson to be :

$$M_Z = 91.9 \pm 1.3 \pm 1.4 \text{ GeV}/c^2 \quad (2)$$

where the first error accounts for measurement errors and the second for the uncertainty on the overall energy scale.

The rms of this distribution is 2.6 GeV/c^2, consistent with the expected Z^0 width[14] and with our experimental resolution of $\sim$ 3%.

Under the hypothesis of Breit-Wigner distribution we can place an upper limit on its full width

$$\Gamma < 11 \text{ GeV}/c^2 \quad (90\% \text{ CL}) \quad (3)$$

corresponding to a maximum of $\sim$ 50 different neutrino types in the universe[15]

The standard SU(2) $\times$ U(1) electroweak model makes definite predictions on the Z^0 mass. Taking into account radiative corrections to 0 (α) one finds[14]

$$M_Z = 77\ \rho^{-\frac{1}{2}}\ (\sin 2\theta_W)^{-1} \text{ GeV}/c^2 \quad (4)$$

where θ_W is the renormalised weak mixing angle defined by modified minimal subtraction, and ρ is a parameter which is unity in the minimal model.

Assuming $\rho = 1$ we find

$$\sin^2\theta_W = 0.227 \pm 0.009 \quad (5)$$

However, we can also use the preliminary value of the W mass found in this experiment[16]

$$M_W = 81.0 \pm 2.5 \pm 1.3 \text{ GeV}/c^2.$$

Using the formula[14]

$$M_W = 38.5\ (\sin\theta_W)^{-1} \text{ GeV}/c^2 \quad (6)$$

we find $\sin^2\theta_W = 0.226 \pm 0.014$, and using also Eq. (4) and our experimental value of M_Z we obtain

$$\rho = 1.004 \pm 0.052 \quad (7)$$

Back-up slides

Observation of WZ EW process

	SR	QCD-CR	b-CR	ZZ-CR
Data	161	213	141	52
Total MC	199.2 ± 1.4	289.4 ± 1.9	159.2 ± 1.8	44.7 ± 6.4
$WZjj$-EW (signal)	24.93 ± 0.18	8.46 ± 0.10	1.36 ± 0.05	0.21 ± 0.12
$WZjj$-QCD	144.17 ± 0.85	231.2 ± 1.1	24.44 ± 0.29	1.43 ± 0.69
Misid. leptons	9.2 ± 1.1	17.7 ± 1.5	29.7 ± 1.6	0.50 ± 0.32
ZZ-QCD	8.10 ± 0.19	14.98 ± 0.34	1.96 ± 0.08	35.0 ± 5.9
tZ	6.46 ± 0.18	6.56 ± 0.19	36.19 ± 0.45	0.18 ± 0.09
$t\bar{t} + V$	4.21 ± 0.18	9.11 ± 0.23	65.36 ± 0.64	2.8 ± 1.3
ZZ-EW	1.50 ± 0.10	0.44 ± 0.05	0.10 ± 0.08	3.4 ± 1.6
VVV	0.59 ± 0.03	0.93 ± 0.04	0.13 ± 0.01	1.0 ± 1.0

Table 1: Numbers of observed and expected events in the $W^{\pm}Zjj$ signal region and in the three control regions, prior to the fit. The expected number of $WZjj$-EW events from SHERPA and the estimated number of background events from the other processes are detailed. The sum of the backgrounds containing misidentified leptons is labelled "Misid. leptons". Only statistical uncertainties are quoted.

Observation of same-sign WW EW process

	e^+e^+	e^-e^-	$e^+\mu^+$	$e^-\mu^-$	$\mu^+\mu^+$	$\mu^-\mu^-$	combined
WZ	1.7 ± 0.6	1.2 ± 0.4	13 ± 4	8.1 ± 2.5	5.0 ± 1.6	3.3 ± 1.1	32 ± 9
Non-prompt	4.1 ± 2.4	2.3 ± 1.8	9 ± 6	6 ± 4	0.57 ± 0.16	0.67 ± 0.26	23 ± 12
e/γ conversions	1.74 ± 0.31	1.8 ± 0.4	6.1 ± 2.4	3.7 ± 1.0	-	-	13.4 ± 3.5
Other prompt	0.17 ± 0.06	0.14 ± 0.05	0.90 ± 0.24	0.60 ± 0.25	0.36 ± 0.12	0.19 ± 0.07	2.4 ± 0.5
$W^\pm W^\pm$jj strong	0.38 ± 0.13	0.16 ± 0.06	3.0 ± 1.0	1.2 ± 0.4	1.8 ± 0.6	0.76 ± 0.26	7.3 ± 2.5
Expected background	8.1 ± 2.4	5.6 ± 1.9	32 ± 7	20 ± 5	7.7 ± 1.7	4.9 ± 1.1	78 ± 15
$W^\pm W^\pm$jj electroweak	3.80 ± 0.30	1.49 ± 0.13	16.5 ± 1.2	6.5 ± 0.5	9.1 ± 0.7	3.50 ± 0.29	40.9 ± 2.9
Data	10	4	44	28	25	11	122

Table 1: Summary of the data event yields, and the expected signal and background event yields in the signal region before the fit. The numbers are shown for six individual channels and for all channels combined. The WZ background is normalized to data in the WZ control region. The backgrounds from $V\gamma$ production and electron charge misreconstruction are combined in the "e/γ conversions" category. The "Other prompt" category combines ZZ, VVV and $t\bar{t}V$ background contributions. The total uncertainty is computed by varying each source of systematic uncertainty by one standard deviation and adding resulting differences in quadrature.